



When archives are missing, deciphering the effects of public policies and climate variability on the Brazilian semi-arid region using sediment core studies

Marie-Pierre Ledru^{a,*}, Vivian Jeske-Pieruschka^b, Laurent Bremond^a, Anne-Lise Develle^c, Pierre Sabatier^c, Eduardo Sávio Passos Rodrigues Martins^d, Manuel Rodrigues de Freitas Filho^d, Diógenes Passos Fontenele^d, Fabien Arnaud^c, Charly Favier^a, Francisco Rony Gomes Barroso^b, Francisca Soares Araújo^b

^a ISEM Université de Montpellier, CNRS EPHE IRD, Place Eugène Bataillon, 34095 Montpellier, France

^b Department of Biology, Federal University of Ceará – UFC, 60440-900 Fortaleza, CE, Brazil

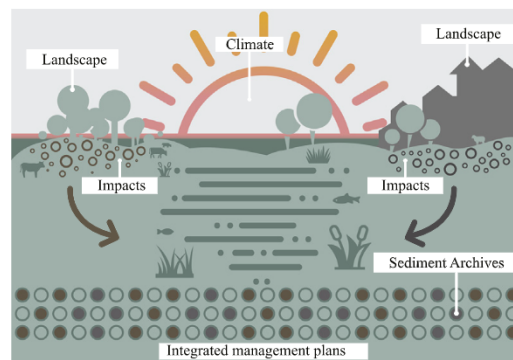
^c EDYTEM, Univ. Grenoble Alpes, Univ. Savoie Mont Blanc, CNRS, 73000 Chambéry, France

^d FUNCEME av Rui Barbosa 1246, CEP 60.115-221 Fortaleza, CE, Brazil

HIGHLIGHTS

- Brazilian semi-arid will face drastic decrease in precipitation in the coming years.
- Archives show both human activities and public policies impact on the resources.
- Ecosystems proved to be resilient to natural climate variability.
- Paleolimnology a good tool to reconstruct the evolution of the landscape
- New management forms account for physical, societal, sustainability specificities.

GRAPHICAL ABSTRACT



ARTICLE INFO

Article history:

Received 26 January 2020

Received in revised form 9 March 2020

Accepted 15 March 2020

Available online 19 March 2020

Editor: Fernando A.L. Pacheco

Keywords:

Caatinga

Lake reservoir

Sediment

Drought

Land degradation

Human impact

ABSTRACT

The northeastern region of Brazil is the most densely populated and biodiverse semi-arid regions of the planet. Effects of the natural climate variability and colonization on the landscape have been described since the beginning of the 16th century but little is known about their effects on natural resources. Climate projections predict temperatures above 40 °C and an increase in the number and duration of droughts at the end of the 21st century with strong societal impacts. Here, we analyze the influence of public policies, human activities and natural climate variability on the environment over the last 60 years. Our study is based on sedimentological and environmental reconstructions from two sediment cores collected in two dam lakes on the river Acaraú in the State of Ceará. Multiproxy analyses of both cores (inorganic geochemistry, pollen, charcoal, remote sensing) at an annual resolution showed that 1) at interannual scale composition and distribution of the dry forest (known as Caatinga) were not affected by the alternance of drought and high moisture episodes; 2) at decadal scale human activities such as agriculture were reflected by changes in vegetation cover and fishery by progressive changes in lake trophic status; 3) public policies were able to promote changes in the landscape e.g., land colonization with the regression of the dry forest and irrigation plan able to amplify the deforestation and change the floristic

* Corresponding author.

E-mail address: marie-pierre.ledru@ird.fr (M.-P. Ledru).

composition. Thanks to paleo-science approach, our environmental diagnosis should help future decision-making and provide guidelines for preservation of resources and wellbeing of the inhabitants.

© 2020 Elsevier B.V. All rights reserved.

1. Introduction

The Brazilian semi-arid (BSA) is the world's most densely populated semi-arid region with >54 million inhabitants. It also hosts 1500 plant, 178 mammal, 591 bird, 177 reptile, 79 amphibian, 241 fish and 221 bee species (Ministerio do Meio Ambiente, 2007) that mostly live in the dry deciduous forest biome known as *Caatinga*. The combination of rainfall variability and intensive land use will make this region one of the world's most vulnerable to climate change in the coming century (IPCC Climate Change Synthesis Report, 2014). The rainfall regime has been highly variable since the 16th century with successive periods of high precipitation and droughts. For example, 48 drought episodes have been reported of which 19 lasted two years or more, and in 1958, millions of people were obliged to flee starvation (Marengo and Bernasconi, 2015). Climate variability, deforestation, the creation of pastureland, irrigation, extensive farming activities, mining since the 17th century (Neto, 2012) and, more recently, overpopulation, have encouraged desertification (Centro de Gestão e Estudos Estratégicos, 2016). Brazilian policies in the 20th century attempted to halt this process through several land use initiatives and recovery of degraded areas (Centro de Gestão e Estudos Estratégicos, 2017) although such projects were often limited to a single region, one such example being "The Caatinga protected areas program" (Portuguese acronym UCCA) developed by the Environmental Municipal Agency for a single municipality. About 447 reservoirs were built with a total capacity of 30,261 hm³ although today they only function at 18% of their capacity (<https://olhonagua.insa.gov.br>).

Since the beginning of the 21st century, in addition to natural variability and anthropogenic land use change, ongoing climate change is again challenging the BSA. Both global and regional climate change scenarios suggest rainfall deficits and increased aridity will prevail in the region by the second half of the 21st century (Marengo and Bernasconi, 2015). Aware of these risks, the Brazilian government set up the "Recovery of degraded areas and reduction of climate vulnerability" (Portuguese acronym URAD) initiative to address the control of the main drivers of land degradation in the Caatinga biome.

Land cover is a common proxy for the long-term impacts of climate change and land use (Lebel et al., 2018). For an integrated assessment of the driving forces likely to affect the landscape, data are collected in field surveys (Ferrenberg et al., 2015), from agricultural yields, and from aerial photographs (Barbosa and Kumar, 2016), as the latter provide an accurate view of the effects of forcing on a landscape and can distinguish anthropogenic from natural forcing in one or several specific time windows (IPCC, 2018). However, in the BSA, the scarcity and the irregularity of such data make it impossible to analyze these effects on the landscape, thereby preventing the production of the crucial information required to take sustainable resource management decisions. Moreover, field surveys do not allow continuous long-term observations (at the scale of several decades) that would be necessary to account for the impacts of current and future climate change when evaluating the future ecosystem services provided by this semi-arid biome. When such archives are absent, sediment cores from lakes (e.g. Levine et al., 2012) or reservoirs (Cardoso-Silva et al., 2016) are commonly used to reconstruct the chronology of pesticides (Sabatier et al., 2014), organic pollutants (Zhang et al., 2019), trophic history (Levine et al., 2012) to estimate degradation and propose some alternatives. However these studies do not inform about total landscape and environmental histories. Here to evaluate the combined effects of public policies, human activities and natural climate variability on the total environment and landscape we

aim testing a new approach based on multiproxy analyses geochemistry and biological proxies crossed with the instrumental data and the launching of the main public policies and, evaluate how well the sediment cores are able to reconstruct an integrated history of the landscape in the BSA (Appendix A).

For our analysis, we proposed an approach based on indirect reconstructions and produced continuous data from archives retrieved from reservoir sediments, using paleolimnological techniques. Multiproxy analyses (sedimentological, geochemical, pollen, charcoal) associated with a chronology based on short-lived radionuclides were performed to characterize the signature of both climate variability and land use in the landscape continuously over time. The aim of the paper is two-fold. Firstly, to test a new approach for historical reconstruction of a landscape in the absence of archives. Secondly, to provide reliable data to understand the changes in landscape resources in recent decades in order to enable policy makers to incorporate these factors to insure the sustainable development of the region.

2. Study area

2.1. Acaraú-Mirim and Araras dams

Our study focused on two dam reservoirs, Acaraú-Mirim and Araras, located in the hydrographic basin of Acaraú, which covers 10% of the total surface area of the State of Ceará with 15 dams along the Acaraú River alone (Fig. 1). The Acaraú River is 320 km long, its headwaters are in the Serra da Mata (700 m asl) near the city of Monsenhor Tabosa and the river flows into the Atlantic Ocean. The Acaraú-Mirim reservoir (03°30.268'S; 40°16.766'W) (ACA) is located in the district of Ipaguacu, 84 m asl, at the foot of the Serra de Meruoca that feeds the dam; the dam spillway feeds the Acaraú River just below the dam. The montane is covered with a dense seasonal deciduous (*Caatinga*) and semi-deciduous forest. Annual precipitation at Meruoca (990 m asl) is 1400 mm. The dam has a capacity of 52,000,000 hm³ and is used to supply the city of Massapê and farms in the vicinity with water for irrigation and fishery activities (Gurgel and Fernando, 1994). The Araras reservoir (04°12.559'S; 40°27.254'W) (ARA) (183 m asl) is located in the seasonal tropical deciduous forest landscape in the district of Varjota and provides water for ~141,000 people. Mean annual precipitation is 880 mm. The dam has a capacity of 891,000,000 hm³ and is intended to supply drinkable water to three cities and their surroundings, as well as water for intensive irrigation (Araras Norte Project), local irrigation and fishery. These reservoirs normally capture a large volume of water during the rainy season, which is irregular in intensity and duration because of the complex climatic pattern (Marengo and Bernasconi, 2015).

2.2. Climate

Between 1990 and 2010, mean annual rainfall in the Acaraú basin was 913 mm. For 45% of the period, annual rainfall was above the mean and for 15% of the period, annual rainfall was below the mean. Rainfall is concentrated between March and May. Thirteen drought events have been recorded in the BSA region in the last 60 years: 1958, 1966, 1970, 1976, 1979–1981, 1982–1983, 1992–1993, 1997–1998, 2001–2002, 2005, 2007, 2010, and 2012–2015 (Alexander et al., 2018; Marengo and Bernasconi, 2015). The February–May rainy season in BSA in 2012 was the driest between 1961 and 2012, and the two driest years since 1961 were 1982 and 2012. During the dry/wet

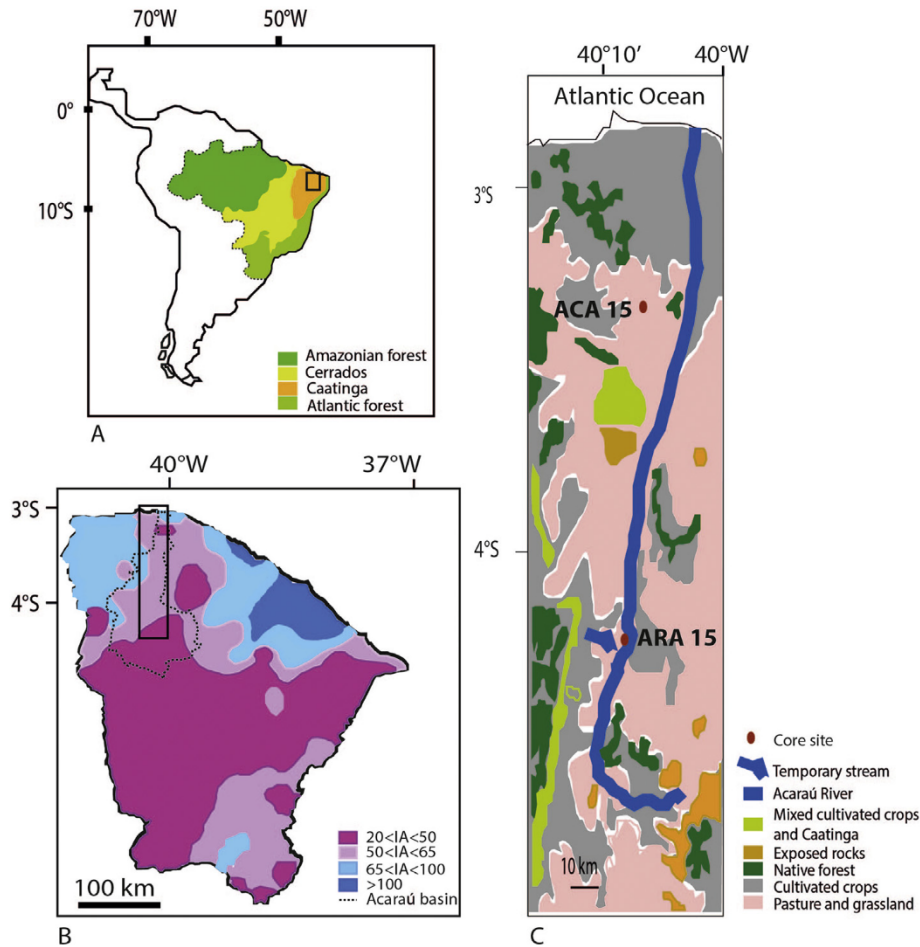


Fig. 1. Location of the study area. A) Map of South America showing the four main Brazilian biomes. B) Map of the State of Ceara in Brazil with the hydrographic basin of the River Acaraú (in grey). C) Representation of the landscape of the Acaraú basin (data from <http://funceme.org>) with the location of the two sediment cores ACA and ARA.

years, inter hemispheric gradient is steep and the ITCZ stays in a northern/southern position while the SST of the equatorial Pacific is anomalously warm/cold. Model predictions show a scenario with a warmer SST in the northern Atlantic, less rainfall and warmer temperatures in the BSA.

The climate of the mountain area near ACA is moister than the inland climate at ARA due to the relief and the proximity of the ocean. Consequently, differences in rainfall anomalies are observed between our two sites. ACA with 1400 mm rainfall per year is less sensitive to drought than the whole hydrographic basin comprising Acaraú and ARA.

At ACA, the driest years were 1983, 1992–93, 1997–98, 2005 and 2012–2015. High moisture rates were recorded in 1985, 1994 and 2009.

At ARA, monitoring started in 1987. The driest years recorded were 1992–93, 1997–98, 2012–2015 and the wettest years were 1989, 1995 and 2009. Considering the Acaraú hydrographic basin as a whole, the driest years were 1979–83, 1992–93, 1998, 2012–2016. Based on these observations, the year 2005 was considered “dry” only at ACA, near the coast. Correlations with the Pacific Decadal Oscillation (PDO 1900–2013) anomaly show that it was negative during the driest years: 1992, 1997–2003, and 2011–2013, while no correlation was observed with the AMO anomaly. A negative anomaly in tropical North Atlantic SST was observed in 1970–75, 1982–84, 1992–93 and in 1997–98 a sharp decrease was observed but the anomaly remained positive. Another correlation between SST and rainfall is observed when considering the SST gradients between tropical North and South Atlantic, the interhemispheric SST dipole, with the driest/wettest years when the S/N Atlantic SST was colder/warmer. Indeed, Northeastern Brazil is

one of the key regions that are severely affected by the meridional mode of tropical Atlantic SST variability (Alexander et al., 2018). During at least the last 50 years, the changes in SST have been closely correlated with rainfall variability.

2.3. Vegetation

The Caatinga dominium is one of the three arid and semi-arid cores of the South American continent (Andrade-Lima, 1981). The Caatinga dominium is a mosaic of tropical thorn woodland and very dry thorn forest at altitudes below 500–600 m asl and dry forest at higher altitudes (sensu the Holdridge life zone ecology). The phytogeographic classification system of Brazil is called savanna-stepic (IBGE, 2010) and represents the dryland biome in Brazil. It is located in northeastern semi-arid region, which occupies 11% of the country with an area of about 1.3 million km². Delimitation was based on rainfall, mean annual rainfall below 800 mm, aridity index up to 0.5, and risk of drought >60% relative to the 1970–90 climatology (Joly et al., 1999). Despite the semi-arid physiognomy, the Caatinga hosts high biomass and high biodiversity.

Four main types of tropical vegetation (Holdridge, 1967) are observed in the Acaraú River Basin: very dry thorn forest (Caatinga) and three types of seasonal dry forests on the slopes and tops of mountains (deciduous, semi-deciduous with babaçu and evergreen forest). The dominant ecosystem is the very dry thorn forest or Caatinga associated with stony impermeable crystalline soils adapted to hydric deficiency. At Acaraú, the Caatinga has been severely impacted by human activities and hotspots of ongoing desertification.

Intensive cotton crops, introduction of grazing in the 16th century in the Acaraú Basin and wood cutting have greatly modified the Caatinga. The degradation of the arboreal Caatinga led to expansion of the shrubs and grasses observed today. The limiting factors for agriculture, i.e. the climate, shallow soil, stony surface, hydric deficiency) obliged the inhabitants to practice itinerant agriculture, in which the land is abandoned after 2 or 3 years, leaving behind secondary vegetation of no economic value (Araújo Filho, 1997) (Appendix D).

2.4. Ecological indicators

The following species were assigned to the drought tolerant group *Mimosa caesalpiniiifolia*, *M. tenuiflora*, *Piptadenia stipulacea*, *Anadenanthera colubrina*, *Poincianella bracteosa*, *Combretum*, *Myracrodruon urundeuva*, *Spondias*, *Zizyphus joazeiro*. *Mimosa caesalpiniiifolia* is the dominant arboreal taxon in the ecosystem despite being very sensitive to degradation in areas susceptible to desertification. These trees occur naturally in the Caatinga and are one of the main sources of stakes for fences in Northeastern Brazil. Considering the climatic conditions of the Brazilian semi-arid region, *Mimosa caesalpiniiifolia* is assumed to be a fast-growing plant species, and is the wood used as fuelwood and for charcoal production (Albuquerque et al., 2009; Milliken et al., 2018). *Combretum leprosum* is a good pollen producer although not abundant in the vegetation. It grows easily in degraded areas. *Alternanthera*, Poaceae, Cyperaceae, *Mitracarpus* and *Borreria* are common in the herbaceous strata of the Caatinga, including on the margins of the reservoirs.

3. Material and methods

3.1. Coring

Two sediment cores were collected in two reservoirs, Acaraú Mirim (ACA) and Araras (ARA) with a gravity corer UWITEC pushed into the sediment in a stable area of the reservoir where the height of the water column was between 6 and 7 m, to guarantee permanent water. The ACA 15-2 core went down to a depth of 97 cm. The ARA 15 core went down to a depth of 60 cm. Cores were split in half using a cutter and a thin metal wire. One half core was kept intact and sent to the EDYTEM laboratory in Chambéry, France for XRF analyses the other half, used for proxy analyses, was cut into 1-cm thick sections, that were immediately placed in plastic bags for storage and kept refrigerated in the laboratory until processing and analysis. Proxy analyses were performed on alternate 1-cm samples.

The base of core ACA 15-2 is composed of compact organic sandy clay up to 80 cm, a layer of fine dark clay between 80 and 77 cm, and fine brown organic clay to the top of the core. The ARA 15 core is composed of fine organic clay with loose wet sediment in the top 10 cm. To define an age depth relation for each core, 13 samples from ACA and 11 samples from ARA were sent to *Laboratoire Souterrain de Modane* France for short-lived radionuclide measurements.

3.2. Dating

^{210}Pb , ^{226}Ra , and ^{137}Cs activities were determined using planar Broad-Energy Germanium (BEGe) detectors placed at the *Laboratoire Souterrain de Modane* following (Reyss et al., 1995) on 1- to 3-cm-thick samples with 12 samples on ARA15 sediment core and 10 samples on ACA15 sediment core. The levels of ^{226}Ra activity were determined using its short-lived daughters ^{210}Pb (295- and 352-keV peaks) and ^{214}Bi (609-keV peak), assuming secular equilibrium with ^{226}Ra . ^{210}Pb (22.3 y), ^{241}Am (432.2 y), ^7Be (53.4 d), and ^{137}Cs (30.2 y) activity levels were directly measured by their gamma emissions at 46.5, 60, 477, and 662 keV, respectively. Excess ^{210}Pb activity was calculated by subtracting ^{226}Ra -supported activity from total ^{210}Pb activity.

3.3. Sedimentological and geochemical analyses

The grain size distributions of core ACA15 were determined using a Malvern Mastersizer S (EDYTEM lab) at a 1 cm continuous interval. After inserting the bulk sediment into the granulometer, ultrasound was applied to minimize particle flocculation. Core ACA15 was also sampled at 1-cm steps and dried at 60 °C during 4 d to obtain its dry bulk density, and then the LOI of each sample was measured using the protocol of Goldberg (1963) and Heiri et al. (2001). The LOI at 550 °C and 950 °C corresponds to the organic and carbonate components of the sediment, respectively.

The relative concentrations of major elements were analyzed on the surface of the sediment core by X-ray fluorescence (XRF) at high resolution (5 mm sampling step) with an Avaatech Core Scanner (EDYTEM Laboratory, CNRS-University Savoie Mont Blanc). The X-ray beam was generated with a rhodium anode and a 125- μm beryllium window, which allows a voltage range of 7–50 kV and a current range of 0–2 mA. Element intensities were expressed in counts per second (cps). Geochemical data were obtained with different settings depending on the elements analyzed. They were adjusted to 10 kV and 1 mA for 20s to detect Si, Ca, Al, Fe, Ti, K, Mn, and S. For heavier elements (i.e. Sr, Rb, Zr, Br, and Pb), measurements were performed at 30 kV and 0.75 mA for 30 s (Jansen et al., 1998). Identification of relationships between element depth-series, the data on each core was subjected to principal component analyses (PCA) using vegan package (Oksanen et al., 2018) on the R platform (Bruel and Sabatier, 2020).

3.4. Pollen analyses

Pollen analyses were performed at 1 cm intervals on 76 samples from ACA and 50 samples from ARA. *Lycopodium* spikes were used to estimate pollen concentrations (Stockmarr, 1971). The samples treatment followed standard protocol (Faegri and Iversen, 1975; Kümmel and Raup, 1965). A minimum of 300 terrestrial grains were counted per sample. Pollen grains and spores were identified using the reference pollen collection of about 130 Caatinga taxa held at the Prisco Bezerra Herbarium of the Federal University of Ceará, and several pollen atlases (Miranda and Andrade, 1990; Oliveira and Santos, 2014; Radaeski et al., 2013; Salgado-Labouriau, 1973; Silva et al., 2016; RCPol).

3.5. Burning biomass

The two cores (ACA 15 and ARA 15) were sampled continuously in each 1-cm layer for the charcoal analyses and prepared using the following steps: (1) Samples were soaked in 5% KOH solution; (2) particles were deflected and bleached in a 10% NaOCl solution; (3) 160- μm mesh was used to separate microscopic coal particles; and (4) microcharcoals were analyzed under a stereomicroscope and using the image analysis software WindSeedle (Umbanhowar and McGrath, 1998).

3.6. Sea surface temperature

Sea surface temperature (SST) data were taken from the NOAA's Extended Reconstructed Sea Surface Temperature, version 4 (ERSSTv4) dataset (Boyin et al., 2015.), available on $2^\circ \times 2^\circ$ global grids, for the years 1950–2017. In order to examine the role of SST, we computed an index of area-averaged SST anomalies within the northern Tropical Atlantic (1° – 20° N, 48° – 20° W) for the December–February season. Anomalies are relative to the 1981–2010 monthly average.

3.7. Remote sensing

We selected the LANDSAT images with the lowest cloud cover index between the years 1973 and 2016. The images were analyzed and interpreted using the functions available in a Geographic Information System (GIS) software for vector editing, cartographic projection

conversion and digital image processing. All images were redesigned for the UTM projection, SIRGAS 2000 datum, zone 24 of the southern hemisphere.

4. Results

4.1. Age model

A chronological framework was established using short-lived radionuclides measurements. The ^{210}Pb excess profiles were plotted on a logarithmic scale (Fig. 2a) and we applied the Constant Flux Constant Sedimentation model (CFCS) (Goldberg, 1963) for our age model. For

ACA 15 we obtained a mean accumulation rate of $13.8 \pm 2.25 \text{ mm}\cdot\text{yr}^{-1}$ and the base of lake sediment dated to $1963 \pm 8.5 \text{ yr AD}$. For ARA15, the ^{210}Pb excess profile (Fig. 2b) showed a regular decrease interrupted by drops in ^{210}Pb activity. Following Arnaud et al. (2002), the low values of ^{210}Pb activity were disregarded for the construction of the synthetic sedimentary record, because the values are related to sedimentary facies that are considered to be instantaneous deposits (Fig. 2b) illustrated by an increase in Si content, corresponding to facies 2. Plotted on a logarithmic scale, the ^{210}Pb activity vs corrected depth revealed a linear trend. Applying the CFCS model, we obtained a mean accumulation rate of $7.17 \pm 1.45 \text{ mm}\cdot\text{yr}^{-1}$. Ages were then calculated using the CFCS model applied to the original

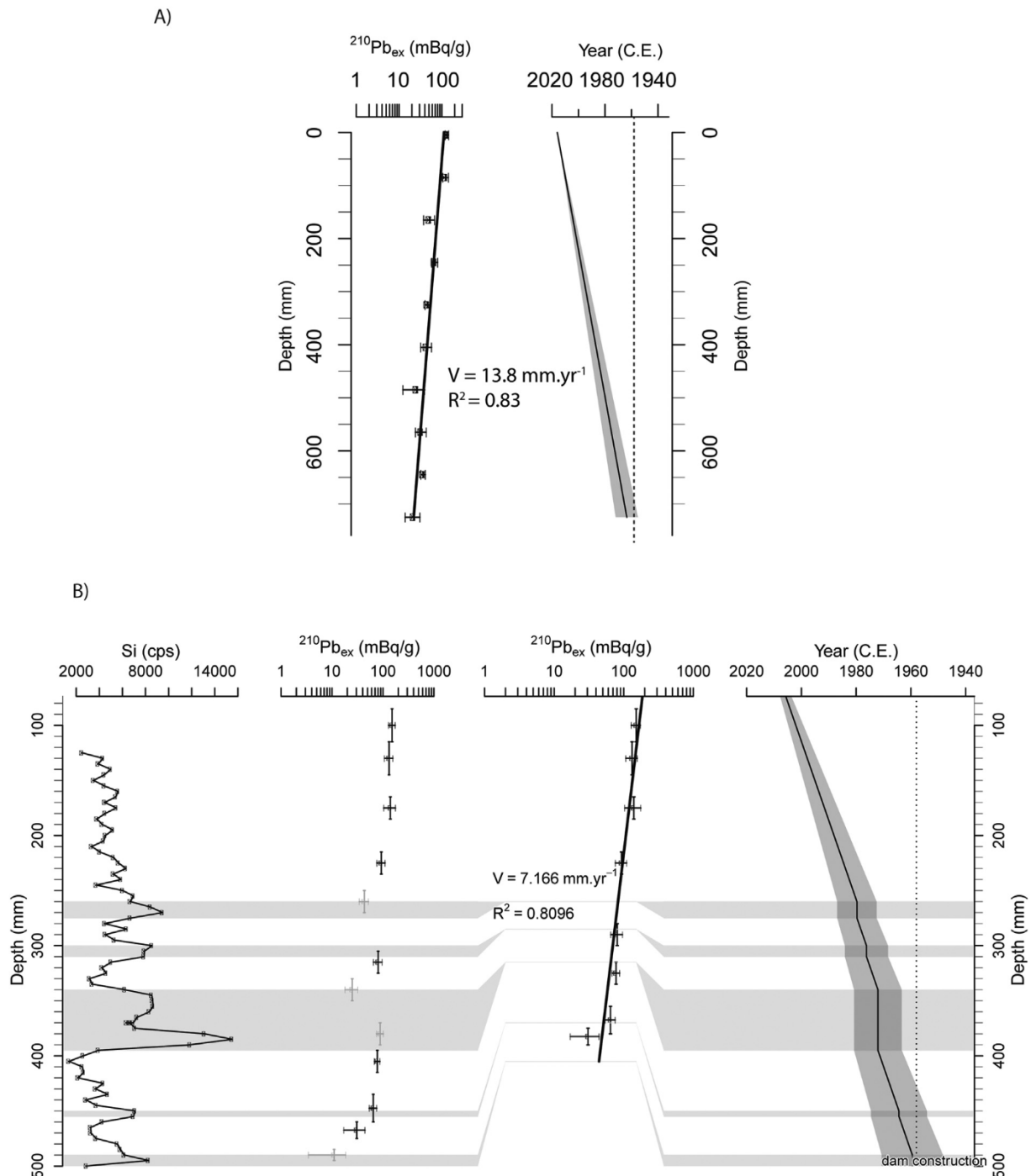


Fig. 2. Presentation of the age model. ^{210}Pb ex activities for (A) the ACA and (b) ARA cores. For ARA, Si contents illustrate high terrigenous content related to high rainfall events that were considered as instantaneous events and removed for age modelling (grey bands).

sediment sequence to provide a continuous age–depth relationship and an age interval of the four instantaneous deposits corresponding to facies 2 (1980 ± 7 yr AD, 1976 ± 8 yr AD, 1972 ± 9 yr AD, 1964.5 ± 10.5 yr AD). The base of the lake sediment (facies 1 and 2) dated to 1959.5 ± 11.5 yr AD in good agreement with the dam construction in 1958 CE. Values for ^{137}Cs activities were under the limit of detection in both cores.

4.2. Depositional environment

Color, grain size, loss on ignition (LOI), and sedimentary structure of the sediments in the reservoir (Figs. 3, 4, 5) allowed to identify three different sedimentary facies in both cores. A brown to green fine-grained sediment (facies 1) in the upper part of both cores (0–74.5 cm in ACA15; and 0–45.5 cm in ARA15), a grey fine-grained sediment (facies 2) interbedded at different depths in facies 1 and a brown coarse sediment (facies 3) at the base of each core (95.5–74.5 cm in ACA15;

60–45.5 cm in ARA15). At ARA, the top 10 cm of the record was a mixture of sediments/water interface and was considered as a single sample.

PCA variables and individual projections highlighted the correlation between different elements in the two cores (Fig. 3). Dimensions 1 and 2 (hereafter Dim1 and Dim2) represent 71% and 78% of the total variance for ARA15 and ACA15, respectively (Fig. 4). In both lakes, the ordination of variables among the first two axes are quite comparable and identify the same main factors of variations, probably linked to the common geological context and origin of the lakes. Three main chemical end-members or units were identified (Fig. 3). The first one was positively correlated with Dim1 and yielded high positive loadings for major terrigenous elements such as K, Zr, Sr and to a lesser extent Ca in both cores, plus Rb in ARA15, and plus Si in ACA15. The second pole with negative loadings on Dim1 made it possible to differentiate Br, S, Mn probably linked to in-lake processes: organic matter (Br) and changes in oxic/anoxic conditions (Mn) in the lake system. The third

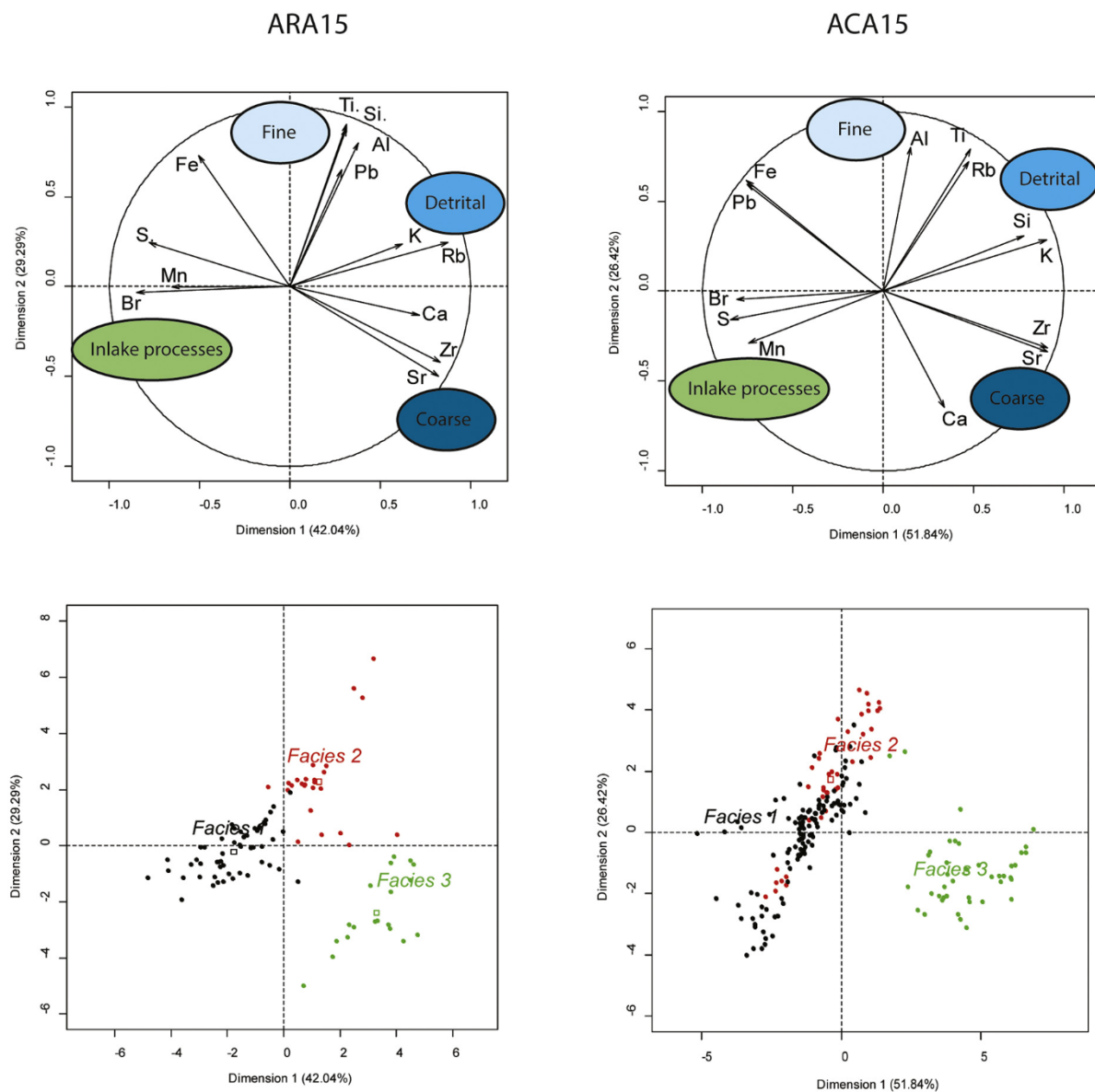


Fig. 3. Definition of the facies. Principal component analyses (PCAs) of geochemical (XRF) data in the ARA15 (left panels) and ACA15 cores (right panels). Upper panels display correlation circles for each PCA in the plan 1–2, with interpretations of each group of elements as representative of inlake process/organic sediment; generic detrital sediment; fine- and coarse-grained detrital sediment. Lower panels represent the loadings of each sample in the plan 1–2, colored according to the sedimentological facies they belong to: black dots, facies 1, brown to green organic rich fine-grained sediment; red dots, facies 2, grey fine-grained sediment; green dots, facies 3, brown coarse sediment.

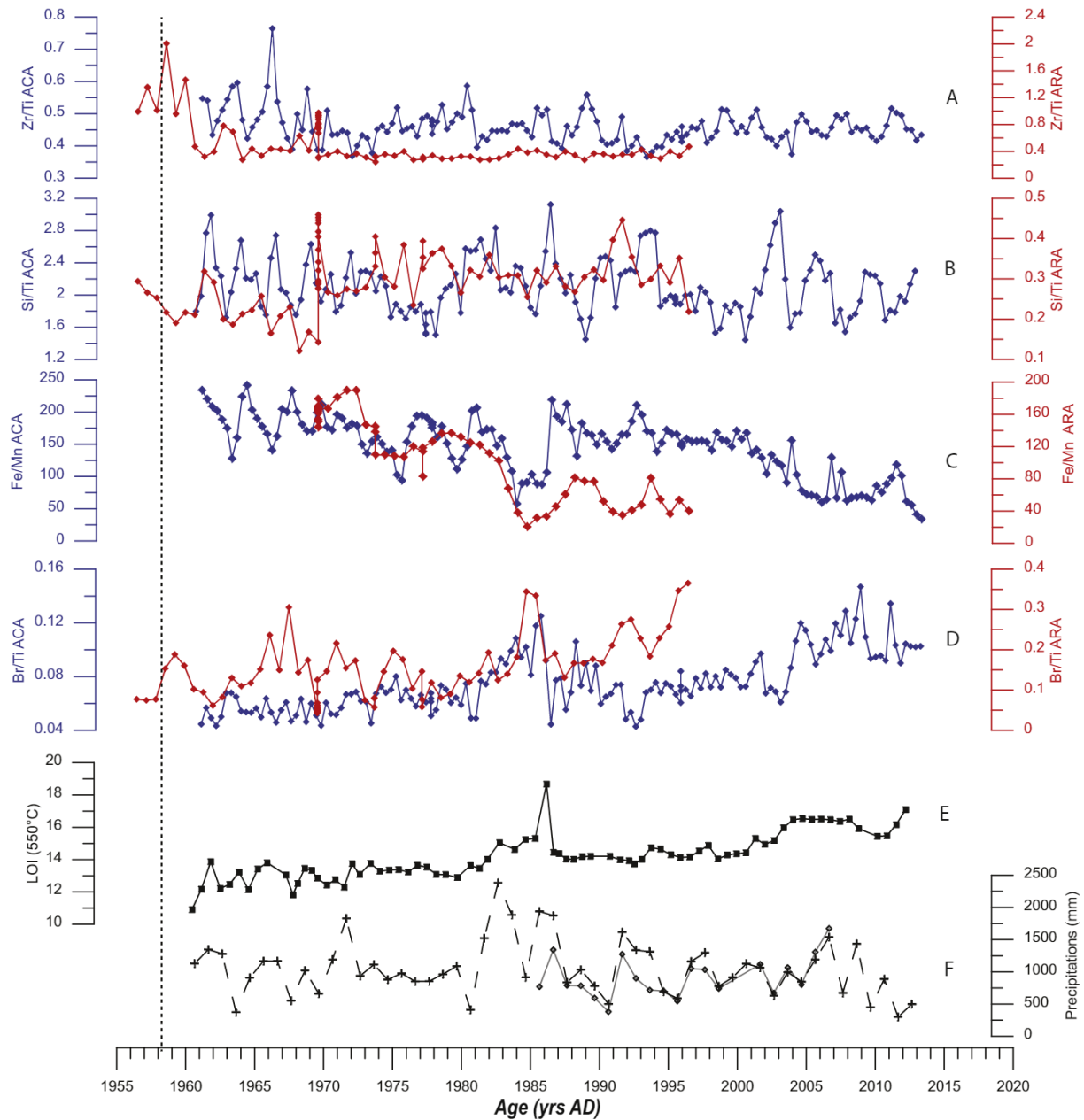


Fig. 4. Downcore geochemical variations. Results for ARA15 (red curve) and ACA15 (blue curve) are plotted against time. The elements plotted here represent the processes highlighted by principle component analysis (Fig. 3). A) Zr/Ti represents sedimentation before the dam was constructed and Si/Ti (B) identifies erosive events after the dam was finished. Fe/Mn (C) has been added to highlight redox processes and Br/Ti (D) was used as a proxy of organic matter content. LOI550 (E) has been added to show the covariation between LOI550 and bromine. Finally, these all proxies are compared with annual precipitation rates in the Acaraú basin, Ipaguassu station close to ACA (dashed line) and Varjota station (full line) near ARA (F).

end-member with a positive loading on Dim2 included other terrigenous elements: Ti and Al in both cores, plus Si and Pb in ARA15 and Rb in ACA15. We were able to separate the two terrigenous end-members thanks to their grain size, the size corresponding to K, Zr, Sr was related to the sand fraction of the sediment and the one enriched in Ti, Al was related to the fine-grained fraction ($<4\ \mu\text{m}$) of the sediment. Fe was located between organic and the fine terrigenous end-member, probably linked to its redox sensitive behavior. Adding the lithological facies 1, 2 and 3 allowed us to map the geochemical distribution of the data (Figs. 3, 7, 9). Mapping the units in the PCA revealed a clear link between facies 1 and the second end-member related to organic rich sediment (LOI550 °C around 15%) linked to long-term sedimentation in the lake system (Fig. 5). Facies 2 was positively correlated with Dim2 and hence with the fine-grained terrigenous end-member and probably

with the high terrigenous input from the watershed due to erosion during high rainfall events/periods. Facies 3 was positively correlated with Dim1 linked to the coarse sediment at the base of each sediment sequence, probably corresponding to soil sediment that existed before the dam was constructed at each site.

4.3. Reconstruction of the tree cover

The composition of the vegetation was reconstructed from pollen analyses (Figs. 7, 8, 9, 10). Among the tree taxa of the Caatinga *Mimosa caesalpiniiifolia*, *M. tenuiflora*, *Piptadenia stipulaceae*, *Anadenanthera colubrina*, *Poincianella bracteosa*, *Combretum leprosum*, *Myracrodruon urundeuva*, *Spondias* sp., *Zizyphus joazeiro* were assigned to the drought tolerant group (Lima et al., 2018). *M. caesalpiniiifolia*, one of the

Bromine & LOI550 correlation

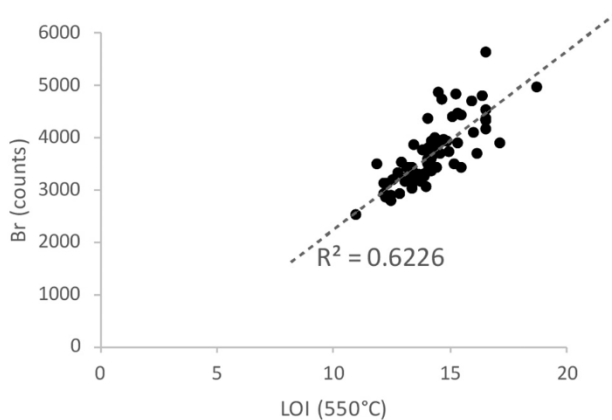


Fig. 5. Graph showing the correlation between Br and LOI in core ACA 15.

dominant arboreal taxa in the Caatinga is very sensitive to degradation (Milliken et al., 2018). *C. leprosum* is a good pollen producer that grows easily although not abundantly in degraded areas (Milliken et al., 2018). *Alternanthera*, Poaceae, Cyperaceae, *Mitracarpus* and *Borreria* are common in the herbaceous strata of the Caatinga (Costa et al., 2007), including on the margins of the reservoirs (Tabosa et al., 2012).

For ACA15, five pollen zones and 81 different pollen and spore types provide evidence for several changes in the landscape during the last 55 years (Figs. 6, 7, Appendix C).

The basal pollen zone (ACA-I, 75–64.5 cm; 11 samples; 1961 to 1969 CE) comprises taxa of the Caatinga with abundant arboreal pollen (27–48%). Fabaceae pollen, mainly *Mimosa caesalpinifolia* (21–44%) and *Mimosa tenuiflora* (0.4–4%), was well represented. Drought tolerant tree pollen taxa ranged from 1% to 6%. This group was represented by *Mimosa tenuiflora*, *Piptadenia stipulacea*, *Anadenanthera colubrina*, *Poincianella bracteosa*, *Combretum leprosum*, *Myracrodruon urundeuva*, *Spondias* and *Zizyphus joazeiro* pollen grains. The herb taxa of the

Caatinga were also well represented. A single pollen grain of *Zea mays* was counted at a depth of 67 cm. Scattered pollen grains belonging to taxa of the seasonal semi-deciduous forest - Serra da Meruoca - were observed in this zone. Aquatic taxa ($\leq 2\%$) and fern spores ($< 2\%$) were scarce. The number of carbonized particles was low and infrequent in this period.

Zone ACA-II (64.5–48.5 cm; 16 samples; 1969 to 1981 CE) was characterized by higher values of tree pollen taxa (44–62%). Although *Mimosa caesalpinifolia* (31–51%) was the most abundant taxon, greater numbers of *Mimosa tenuiflora* (2–10%), *Piptadenia stipulacea* (0.3–3%) and *Senna* (0.3–3%) accounted for the increase in arboreal pollen. Drought tolerant tree pollen taxa reached higher values (5–13%), mostly due to increased percentages of *Mimosa tenuiflora* (2–10%) and *Piptadenia stipulacea* (0.3–3%) pollen. While pollen of *Anadenanthera colubrina* appeared in more samples than previously, percentages of *Combretum leprosum* pollen were still very low (0–1%). Pollen from *Alternanthera* (15–25%) and Poaceae (4–15%) were still well represented, whereas pollen from *Borreria* (2–18%) and *Mitracarpus* (1–4%) declined and both Asteraceae (0–2%) and Urticaceae (0–2%) pollen were still only present at lower proportions. Abundances of Cyperaceae pollen remained stable (2–5%) but both *Cleome* (0–4%) and the aquatic plant *Echinodorus* (0–2%) increased slightly in this zone. The amount of charcoal particles was still low in this zone.

The pollen assemblages of the ACA-III zone (48.5–37.5 cm; 11 samples; 1981 to 1988 CE) were characterized by a significant decrease (from 42% to 16%) in arboreal pollen. NAP taxa of the Caatinga were well represented. Pollen of *Zea mays* ($< 1\%$) appeared more frequently. There was a marked decrease in arboreal pollen, mostly due to the decline in *Mimosa caesalpinifolia* (7–34%). Drought tolerant tree pollen taxa decreased (1–8%), mainly due to the low percentages of pollen of *Mimosa tenuiflora* (0.2–5%) and the low proportions of pollen of *Piptadenia stipulacea* (0–2%) and *Myracrodruon urundeuva* (0–1%). However, while the proportions of *Combretum leprosum* pollen remained low at the base of the zone (0.3%) they increased to 3% toward the top. Dam bank taxa were more abundant (4–12%) than in zone ACA-II, mainly due to higher proportions of Cyperaceae (1–8%) but also *Cleome* (2–4%) pollen. Aquatic taxa ($< 2\%$) were slightly less frequent than in the previous zone. Charcoal particles were very scarce in this period.

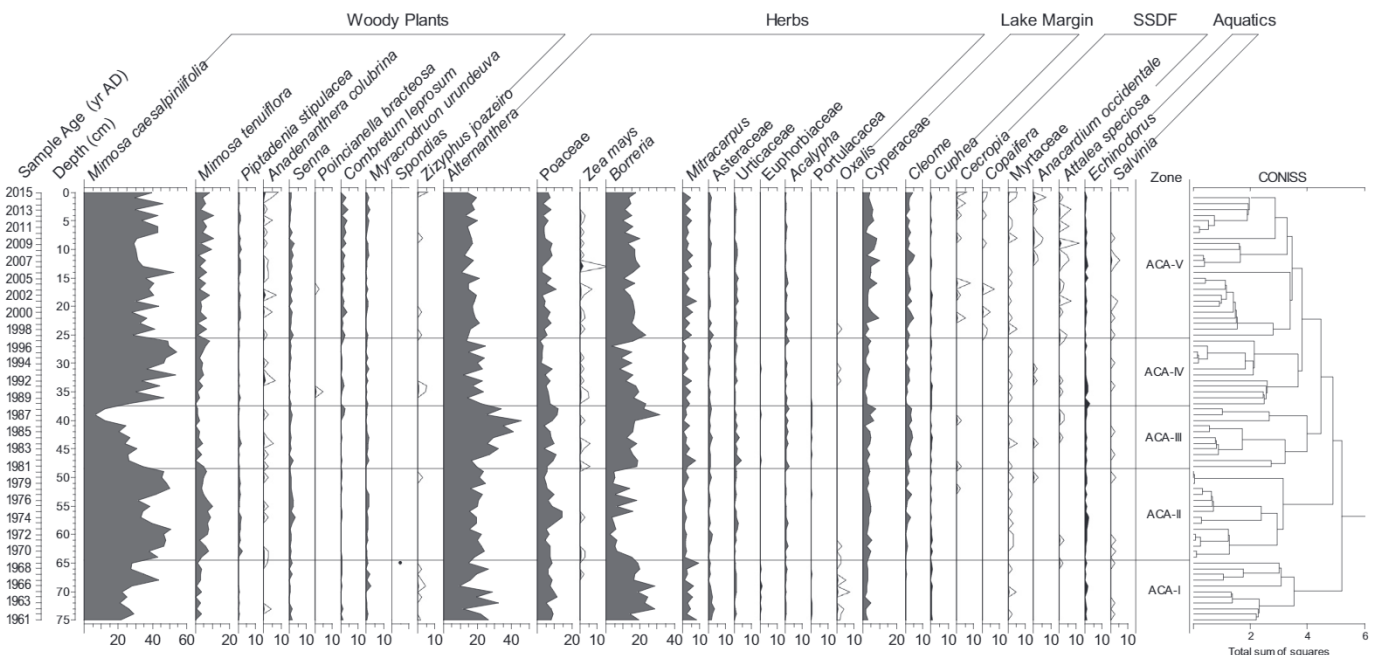


Fig. 6. Pollen diagram of the ACA 15-2 core. Groups of dominant taxa are classified as woody plants, herbs, plants growing on the lake margin, seasonal semi-deciduous forest (Serra da Meruoca) and aquatic plants. Pollen zones were defined based on the results of the cluster analysis. Hollow curves correspond to an exaggeration $\times 10$.

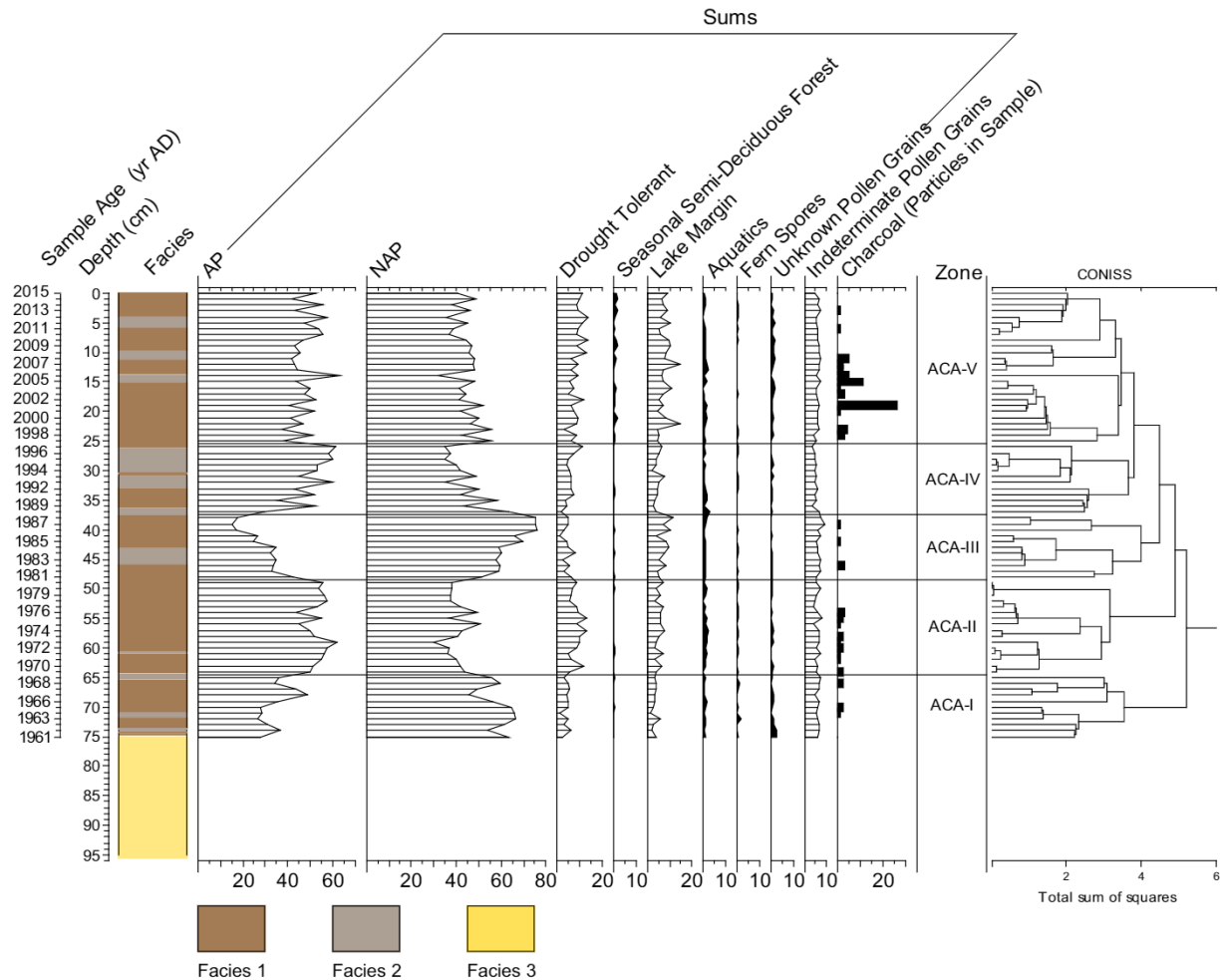


Fig. 7. Summary pollen diagram of the ACA 15-2 core. Representation of the frequencies of ecological pollen groups together with the number of charcoal particles in each sample, as well as the cluster analysis dendrogram. The three lithological units were defined based on the geochemical analyses (Figs. 3, 4).

ACA-IV (37.5–25.5 cm; 12 samples; 1988 to 1998 CE) showed an increasing trend in arboreal pollen abundances (30–61%), whereas the opposite was observed for non-arboreal pollen percentages (35–63%). Arboreal pollen was continuously represented by *Mimosa caesalpinifolia* (26–54%) in which there was a marked increase compared to the previous zone. Among non-arboreal pollen, there was a significant decrease in *Alternanthera* (12–25%), *Mitracarpus* (0–5%), Asteraceae (<2%), Urticaceae (0–2%) and in *Acalypha* (0–2%). Pollen of Poaceae (2–9%), *Zea mays* (<1%) and *Borreria* (4–23%) decreased toward the top of the zone. The increase in the pollen curve for drought tolerant tree taxa (2–11%) was mainly due to higher pollen counts of *Mimosa tenuiflora* (1–9%), but *Piptadenia stipulacea* (<2%), *Combretum leprosum* (<2%) and *Myracrodruon urundeuva* (0–1%) remained low. Pollen of *Poincianella bracteosa* appeared for the first time at 35 cm. Abundances of plant species growing on the dam banks (2–8%) decreased in comparison to the previous zone. No charcoal particles were counted in this zone.

The uppermost pollen zone (ACA-V, 25.5–0 cm; 26 samples; 1998 to 2015 CE) was characterized by stable arboreal (37–63%) and non-arboreal (32–56%) pollen taxa. *Mimosa caesalpinifolia* (28–52%) dominated the arboreal pollen group, while *Alternanthera* (11–21%), Poaceae (3–11%), *Borreria* (10–24%) and *Mitracarpus* (1–8%) accounted for the highest values in the non-arboreal pollen group. Pollen of *Zea mays* (<2%) was still present. Proportions of pollen of drought tolerant tree pollen taxa increased from 3% to 14%. Abundances of *Mimosa tenuiflora* (1–11%) and *Myracrodruon*

urundeuva (0–2%) pollen remained stable, while percentages of *Combretum leprosum* pollen continued to increase (0.3–4%). Pollen of *Piptadenia stipulacea* (0–2%), *Anadenanthera colubrina* (<1%) and *Senna* (0–3%) pollen increased slightly. Pollen of Cyperaceae (2–10%) and *Cleome* (1–6%) reached their highest values in the whole record. The percentage of moist semi-deciduous forest increased to 2% due to higher proportions of pollen of *Cecropia* (<1%), Myrtaceae (<1%), *Anacardium occidentale* (<1%) and *Attalea speciosa* (0–1%). Pollen of Sapindaceae (not shown in the diagram) and *Copaifera* appeared for the first time in this zone. The number of carbonized particles increased markedly in this period, but gradually decreased again toward the top.

For ARA15, constrained cluster analysis divided the pollen diagrams into four main zones (ARA-I to IV) and 74 pollen taxa and four spore types were identified (Figs. 8, 9; Appendix C).

The top 10 cm of the record was a mixture of sediment/water interface and was considered as a single sample. Based on the constrained cluster analysis as well as the 74 pollens and four different spore types identified, the pollen diagrams were divided into four main zones (ARA-I to IV).

Zone ARA-I (60–45.5 cm; 15 samples; before 1960 to 1966 CE) was characterized by high percentages of NAP (62–84%) and low percentages of AP (9–31%). Pollen from drought tolerant tree taxa ranged from 3% to 13%. This group was represented by *Mimosa tenuiflora*, *Piptadenia stipulacea*, *Anadenanthera colubrina*, *Poincianella bracteosa*, *Combretum*, *Myracrodruon urundeuva*,

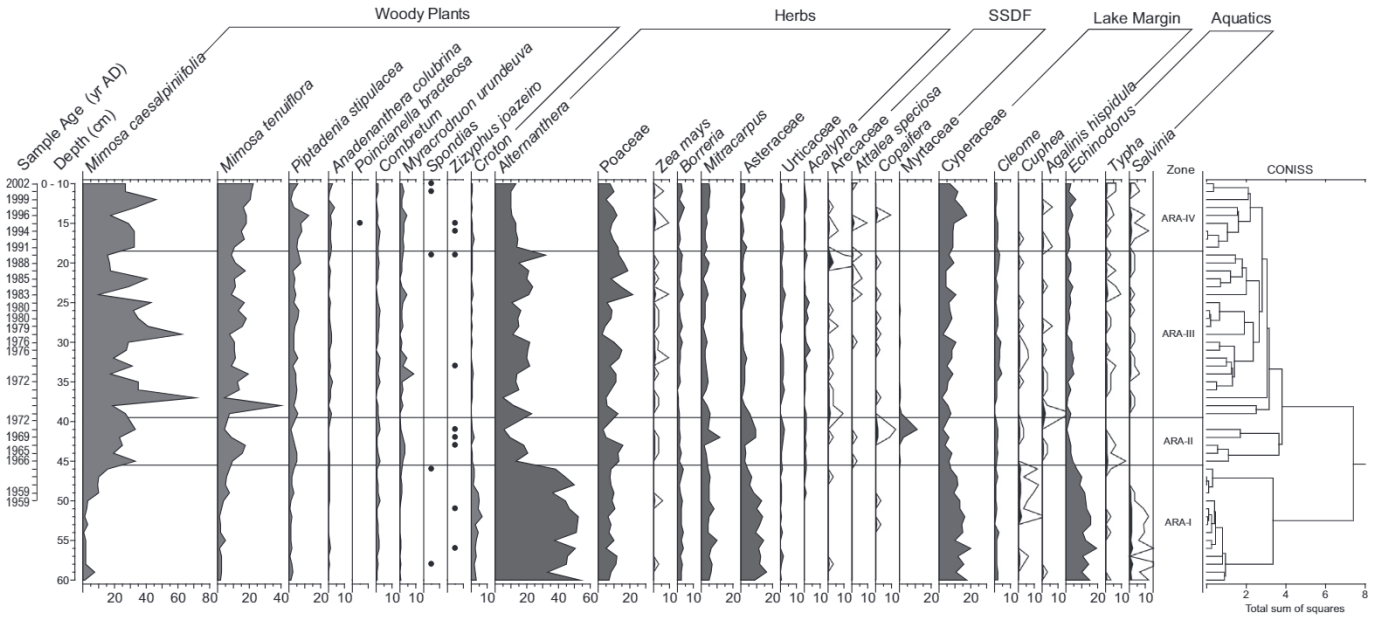


Fig. 8. Pollen diagram of the ARA 15 core. Groups of dominant taxa are classified as woody plants, herbs, seasonal semi-deciduous forest (SSDF) - Serra Ibiapaba plants growing on the lake margin, and aquatic plants. Pollen zones were defined based on the results of the cluster analysis. Hollow curves correspond to an exaggeration x10.

Spondias and *Zizyphus joazeiro* pollen grains. Low abundances of AP were mostly due to lower percentages of *Mimosa caesalpinifolia* pollen (1–16%) and *Mimosa tenuiflora* pollen (1–8%). Pollen of *Croton* reached higher values, between 1% and 7%. The NAP were dominated

by pollen of *Alternanthera* (33–54%), *Poaceae* (5–12%), *Borreria* (1–4%), *Mitracarpus* (4–10%), *Asteraceae* (4–16%) and other herbaceous plants (*Froelichia/Gomphrena*, *Euphorbia* and *Microtea*) not shown on the diagram. Pollen grains of the moist seasonal semi-

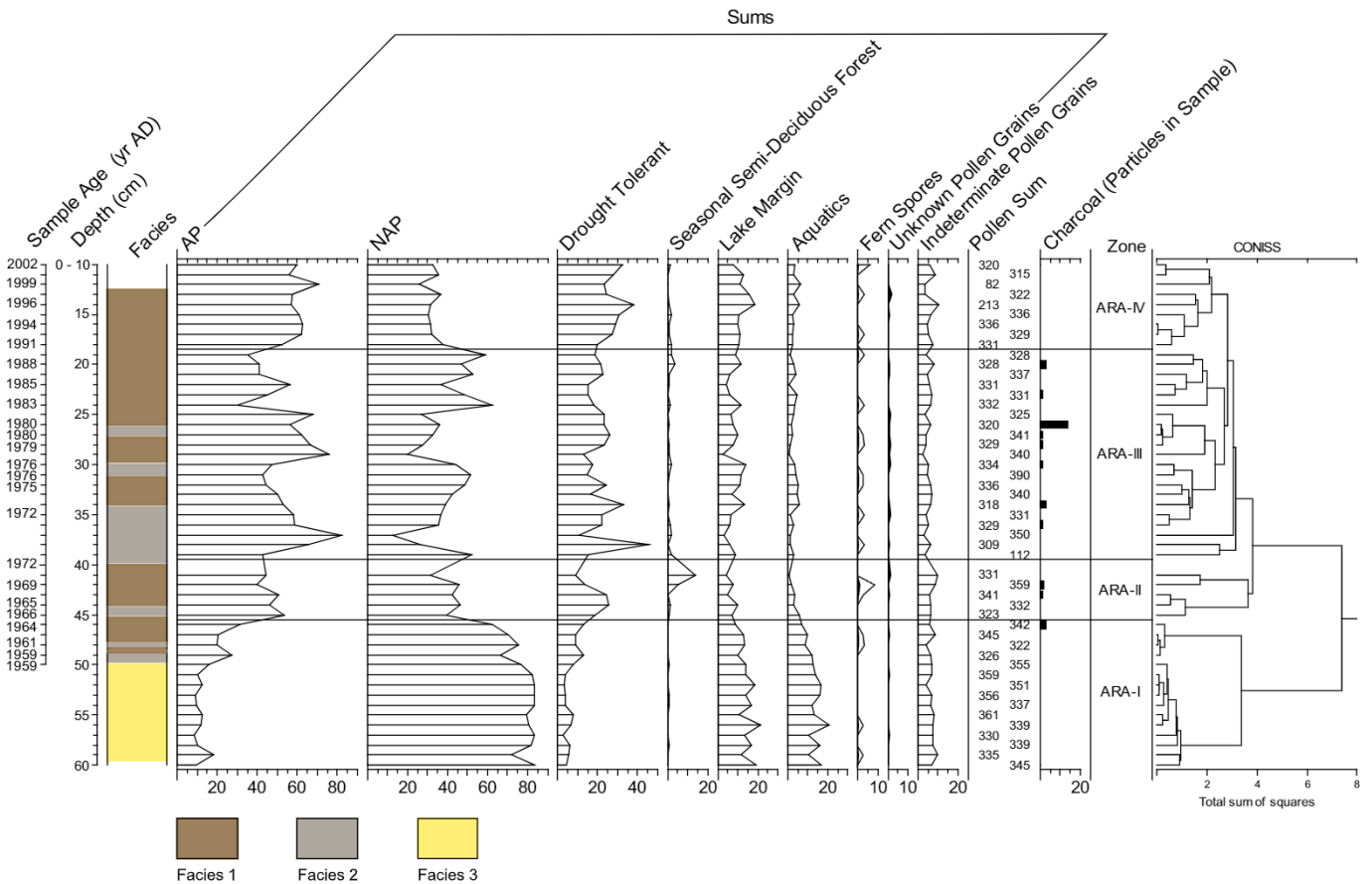


Fig. 9. Summary pollen percentage diagram of the ARA 15 core. Representation of the ecological groups, the number of charcoal particles and the cluster analysis dendrogram. The three lithological units were defined based on the geochemical analyses (Figs. 3, 4).

deciduous forest occurred sporadically. This zone contained high pollen abundances of sedges (Cyperaceae 7–20%) as well as herbs such as *Cleome* (0–2%) and *Cuphea* (0–2%) that grow on the banks of the dam. The aquatic group was well represented by pollen of *Echinodorus* (6–19%) and spores of *Salvinia* (0–2%). Carbonized particles were only present in the uppermost part of the sample. The seasonal semi-deciduous forest group increased up to 14% in this zone, because of higher proportions of Myrtaceae (0–11%) pollen.

Zone ARA-II (45.5–39.5 cm; five samples; 1966 to 1972 CE) was marked by an increase in AP from 40% to 53%, mostly due to an increase in *Mimosa caesalpinifolia* with values up to 33%. The higher representation of pollen from drought tolerant tree pollen taxa, which varied between 9% and 25%, was due to the high pollen frequencies of *Mimosa tenuiflora* (5–17%), *Piptadenia stipulacea* (1–5%) and *Myracrodruon urundeuva* (0.3–3%) while *Combretum* pollen frequencies remained stable (0.3–2%). Abundances of *Croton* (0–2%) pollen decreased in this zone. Herbs, mostly represented by pollen of *Alternanthera* (5–21%), Poaceae (3–15%), *Borreria* (1–2%), *Mitracarpus* (2–12%), Asteraceae (2–10%) and Urticaceae (1–2%) were less frequent. The moist semi-deciduous forest taxa increased to 14% in this zone, because of higher proportions of Myrtaceae (0–11%) pollen. The abundance of herbs growing on the dam banks decreased (4–10%), due to less frequent Cyperaceae pollen (2–8%). The proportion of aquatics (0.6–6%) was lower than in the previous zone due to the decline of *Echinodorus* pollen (0.6–4%) and the absence of *Salvinia* spores. Charcoal particles were observed at depths of 42 and 43 cm.

Zone ARA-III (39.5–18.5 cm; 21 samples; 1972 to 1989 CE) - AP increased continuously from 30% to 82% but then dropped to 35% at the top of the zone. The most abundant arboreal pollens were *Mimosa caesalpinifolia* (10–71%), *Mimosa tenuiflora* (5–40%), *Piptadenia stipulacea* (2–7%), *Anadenanthera colubrina* (0–2%), *Combretum* (0–3%) and *Myracrodruon urundeuva* (0–9%). NAP had a minimum of 13% in the lower part of the zone but increased to 64% toward the top. Among herbaceous taxa, *Alternanthera* (5–32%) and Poaceae (2–22%) pollen were abundant. Pollen of *Borreria* (0–3%), *Mitracarpus* (0.3–5%), Asteraceae (0.3–5%), Urticaceae (0–3%), *Acalypha* (0–4%) and *Zea mays* (<1%) were also well represented. Pollen from drought tolerant tree taxa showed an increasing trend from 11% to 46%. In this zone, taxa from the moist semi-deciduous forest group were represented by lower pollen frequencies, between 0% and 4%, mainly because of very low values of Myrtaceae (<1%). Percentage values of *Attalea speciosa* pollen (<1%) and *Copaifera* (<1%) remained low, whereas Arecaceae (0–3%) pollen grains became more frequent. Taxa that grow on the dam banks also reached higher values, mostly due to increasing percentages of Cyperaceae (2–10%) and *Cleome* pollen (0–4%). Aquatics taxa were represented by increasing *Echinodorus* (0.3–5%) pollen and *Salvinia* (<1%) spores. The amount of microscopic charred particles increased during this period.

Zone ARA-IV (18.5–0 cm; 9 samples; 1989 to 2002 CE) - AP predominated with frequencies ranging from 53% to 71%, whereas NAP decreased, ranging from 26% to 38%. Percentages of *Mimosa caesalpinifolia* pollen remained high (17–46%). The increase in pollen from drought tolerant tree taxa from 20% to 38% was mainly due to higher values of *Mimosa tenuiflora* (10–23%) and *Piptadenia stipulacea* pollen (1–13%). Pollen abundances of *Anadenanthera colubrina* (0–3%) and *Myracrodruon urundeuva* (1–4%) increased slightly, while percentages of *Combretum* pollen (up to 2%) remained low. *Poincianella bracteosa* pollen appeared for the first time at a depth of 15 cm. Herbs were characterized by decreasing values of *Alternanthera* (1–8%) and Poaceae (5–12%), and percentages of pollen from other herbaceous taxa continued to be low. Pollen of *Borreria* (1–4%) and *Mitracarpus* (2–6%) increased in the upper part of this zone. Proportions of seasonal semi-deciduous forest taxa decreased from 2% to 0%. Pollen frequencies of Cyperaceae increased

to 17% while percentages of *Cleome* (<2%) decreased in this zone. Aquatic taxa remained stable at (2–6%). No charcoal particles were counted in this zone.

5. Discussion

5.1. Effects of climate variability

Interannual rainfall variability does not reflect unequivocally in any of both records. Changes in the geochemical proxies Si and Zr identified in facies 2, revealed four terrigenous events in both records although the timing was different, showing an increase in erosion probably linked to either extreme precipitation events or to agricultural activities (Hounsou-gbo et al., 2015; Wilhelm et al., 2012). At ACA15, these events match periods of increased precipitation in the years 1982–83, 1987–88, 1992–96 and 2006–2012, with associated age model uncertainties, that can be clearly observed in the sediment sequence but less in the vegetation composition (Fig. 4). Between AD 1969 and 1981 (pollen zone ACA-II; Fig. 6) there was a significant increase in the tree taxon *M tenuiflora* although this zone includes two climatic intervals: the interval 1969 to 1974 with above normal rainfall, with six months of >50 mm/month, and the interval 1975 to 1980 with below average rainfall (Appendix B). Between AD 1997 and 2015, the arboreal (37–63%) taxa remained stable even though this zone includes the driest phase of the entire study with only two years with consecutive above-average rainfall (1999–2000 and 2008–2009), of which only 2009 had significantly more rain. Over the last 15 years, above average rainfall was only recorded in three years (2008, 2009 and 2011). In the years 2012, 2014 and 2015, the recorded rainfall values resembled those during the severe droughts in 1966 and 1983. But despite several consecutive years of below normal rainfall, rains were well distributed over five to six months with ≥ 50 mm/month (Appendix B) unlike in 2012 and 2015 when the little rain that fell was distributed over three months. In 2014, even with four rainy months, the standard deviation of the annual mean precipitation was the lowest since 1963.

In ARA15, the four observed terrigenous events in 1964.5 ± 10.5 yr AD, 1972 ± 9 yr AD, 1976 ± 8 yr AD, 1980 ± 7 yr AD (Fig. 4) do not match the major reservoir overflows that were observed twelve times between 1978 and 2011 (Figs. 10, 11). Between 1960 and 1980 the tree cover progressively increased either due to the absence of major drought episodes during this interval or to an increase in local moisture due to the construction of the dam (Figs. 3, 10, 11). We observed changes in the vegetation with a sharp decrease in *M. caesalpinifolia* during the 1982 drought followed by re-expansion during the rainy interval in 1984–85 (Fig. 11). Between AD 1990 and 2002, the Caatinga tree taxa increased and showed the highest values of the whole record. No major changes in vegetation were observed during the drought in 1992–1993, whereas a sharp decline in *Piptadenia stipulacea* was observed during the drought in 1998, a decrease in *M caesalpinifolia* was observed during the drought in 2001–2002, whereas *M tenuiflora* continued to expand progressively (Figs. 8, 9, 11). These results show that at the decadal scale Caatinga tree taxa have generally always been well represented irrespective of the mean annual climatic conditions and highlight the resilience of this ecosystem, which is well adapted to the alternance of drought and high moisture episodes. Therefore, rainfall variability was not the primary driver of vegetation and land cover and human activities have to be taken into consideration.

At a multidecadal scale, the progressive increase in tree pollen taxa *C. leprosum* at ACA and *M. tenuiflora* at ARA (Figs. 7, 9) followed the same pattern as tropical Atlantic SST (Fig. 11). Given the close link between SST and climate in the Ceará (Alves et al., 2009; Hounsou-gbo et al., 2015), we can infer that these plant taxa responded to regional

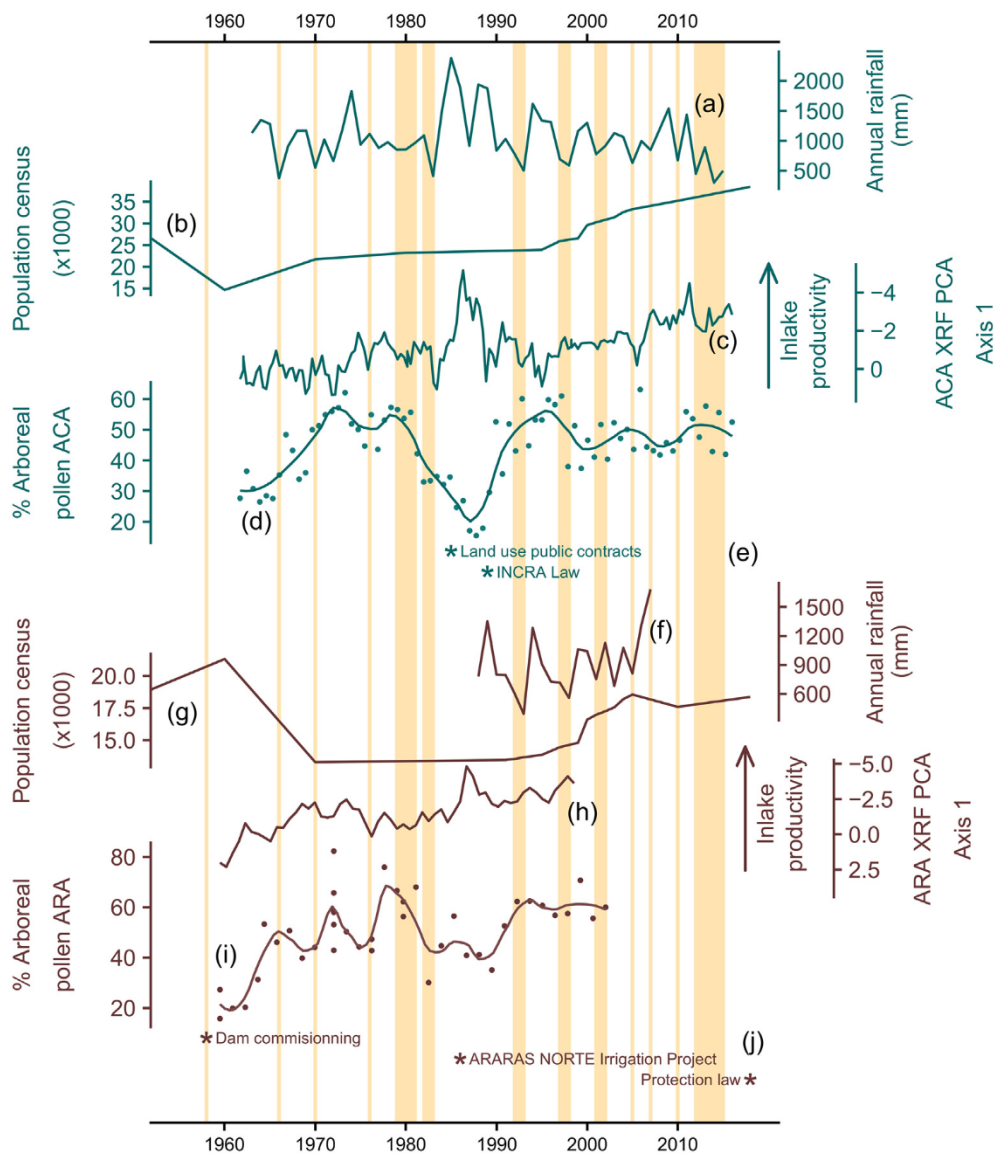


Fig. 10. Main results. In the Acaraú basin A) mean annual rainfall (<http://funceme.org>), B) demography (from the Brazilian institute for geography and statistics IBGE <https://www.ibge.gov.br>), C) in-lake productivity inferred from principal component analysis axis 1 scores (Fig. 3), D) arboreal pollen frequency in core ACA 15, E) launching of public policies in the region of ACA, and in the Araras basin with F) mean annual rainfall (<http://funceme.org>) G) demography (from the Brazilian institute for geography and statistics IBGE <https://www.ibge.gov.br>), H) in-lake productivity inferred from principal component analysis axis 1 scores (Fig. 3), I) arboreal pollen frequency of core ARA 15, J) launching of public policies in the region of ARA. Orange bars identify the drought years.

changes in temperature and/or rainfall. Thus, the internal floristic composition of the Caatinga is likely to evolve progressively as a function of changes in the SST.

5.2. Human impacts

Bromine (Br) in the sediment was associated with organic matter and used as a proxy for organic content (Bajard et al., 2016), confirmed by the correlation between LOI550 and Br contents (Fig. 5) with a similar increase in the upper part of ACA15 around 1987 and since 2003. XRF concentration of manganese (Mn) is an indicator for redox processes and rapid changes in oxic-anoxic conditions at the water-sediment interface (Davison, 1993; Deflandre et al., 2002; Elbaz-Poulichet et al., 2014). Abrupt changes can be caused by flood events that may favor re-oxygenation of bottom water (Wilhelm et al., 2012). In organic rich lake environments with hypoxic conditions caused by the decomposition of organic matter, an increase in Mn may be observed during abrupt re-oxygenation of the sediment/water interface linked to mass movement of water (Wirth et al., 2013). In ACA15, we observed both

indicators (organic matter and oxygenation; Fig. 11) since 2003 suggesting that this lake system experienced a change in trophic status with an increase in in-lake productivity and more hypoxic conditions. Consequently two distinct lacustrine phases were observed: 1) a first one between 1961 and 2003 with fine sedimentation and flooding evidenced by terrigenous material and occasional precipitation of Mn caused by re-oxygenation due to flood events (Wilhelm et al., 2012); 2) a second phase between 2003 and 2015 with a change in trophic status possibly related to the development of fisheries (Gurgel and Fernando, 1994) and to the increase in population around the lake (20% increase between 1999 and 2003) (Figs. 10, 11). Many reservoirs created in the BSA in the second half of the 20th century currently suffer from eutrophication and no longer provide drinkable water (CGEE 2017).

Today, the region around ACA is a vast area of intensive agriculture. Pollen of *Arecaceae*, *Cecropia* sp. (a pioneer indicator of deforestation of the semi-deciduous forest) and *Anacardium occidentale* (cashew) appeared often in the last 20 years, while pollen of *Sapindaceae*, *Copaifera* sp. and *Attalea* sp. (Babaçu a species of palm that produces oil) were

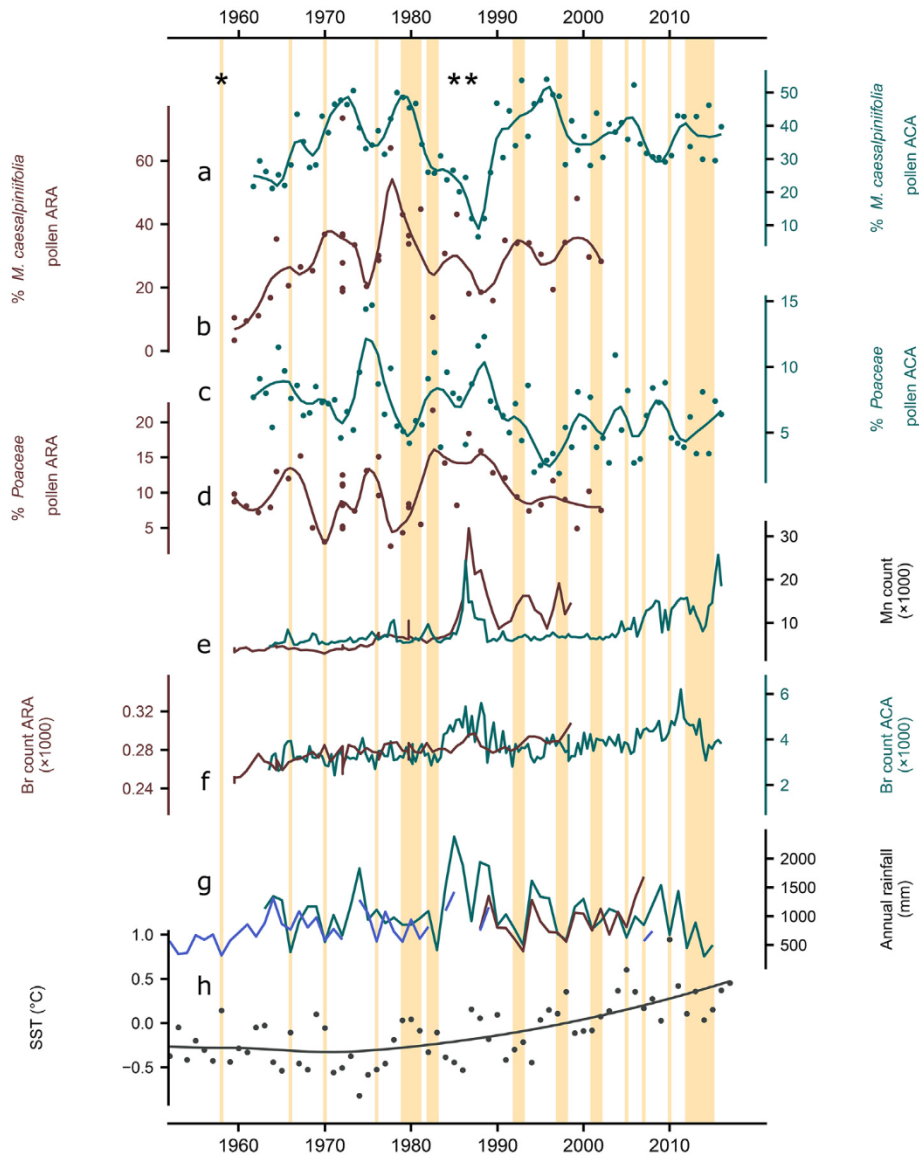


Fig. 11. The last 60 years in the Acaraú region. (A) pollen frequencies of the drought sensitive taxa *Mimosa caesalpinifolia* (B) Poaceae pollen frequencies; in landscape conditions (C) Mn content used as proxy of redox conditions (D) Si content corresponding to terrigenous inputs; in climatic conditions (E) Mean annual precipitation at three meteorological stations: Quixeramobim (blue), Ipaguassu close to ACA (green) and at Varjota (brown) near ARA (<http://funceme.org>) (F) Sea surface temperature for northern Tropical Atlantic (Boyin et al., 2015). Orange bars identify the drought years (3). Asterisks mark the launching of public policies discussed in the text.

found for the first time after 1963. Cashew and native babaçu palm are cultivated in the Serra da Meruoca for commercial purposes (Coradin et al., 2018). Despite the creation of the Serra da Meruoca Environmental Protection Area in 2008 (Law N° 11891), some families continued to practice subsistence farming there.

At ARA local deforestation are shown by the increase in charcoal particles with a peak in 1983 and of cultivated taxa such as *Zea mays* (Figs. 8, 9).

5.3. Effects of public policies

The date of occurrence of the different events discussed below integrates the error interval defined by the age model when comparing with the launching of the public policies (Fig. 2). In ARA, before 1958, when the reservoir was not yet active, low tree pollen frequencies (<5%) characterized a dry open landscape with abundant dry herbaceous taxa (mainly *Amaranthaceae Alternanthera* sp. and *Rubiaceae Mitracarpus* sp.) (Figs. 8, 9). This interval reflects the nature of the

landscape before and during the construction of the dam that started in 1951 and was inaugurated in 1958. The decrease in Zr content, a geochemical indicator associated with coarse element represented by medium sand (facies 3 and Figs. 4, 11) was evidence for the installation of the lacustrine system due to the construction of the dam. After the dam began functioning, the main changes in the vegetation between AD 1963 and 1971 were reforestation with the expansion of the Caatinga tree species mainly *M. caesalpinifolia*, *M. tenuiflora* and *Myracrodruon* sp. and an abrupt decrease in the herb taxa. Two more humid periods in 1987 and 1994 were visible through geochemical proxies (Fig. 11). In 1986, the irrigation law for northeastern Brazil was passed (Lei 10 Setembro 1986 Programa de Irrigação do Nordeste – PROINE) resulting in a significant extension of the cultivated area with, in particular in the hydrologic basin of Varjota, the Araras Norte Project that included 1346 irrigated ha destined for fruit production (Ximenes and Furtado, 2018). The highest concentration of Br recorded in 1987 related to an increase in organic matter in the lake likely due to the erosion of soil litter. The implementation of the irrigation plan was

associated with a sharp prolongation of the local deforestation as evidenced by the decrease in *M. caesalpinifolia* and *M. tenuiflora*, more frequent microscopic charred particles associated with increased burning (Fig. 9) and the expansion of cultivated crops (Fig. 9). Remote sensing reconstructions for the year 1999 show an increase in natural vegetation cover related to high moisture rates while in 2016, after four years of very low rainfall, a significant reduction in vegetation cover and an increase in bare soil emphasize the limits of the above mentioned irrigation plan (Fig. 12).

At ACA, between 1980 and 1988, the vegetation cover became more open with a decline in trees and shrubs, and more particularly in *M. caesalpinifolia* despite years with abundant rainfall after the severe drought of 1982–83 (ACA-III in Appendix B; Figs. 10, 11). Human activities were triggered by the award of public contracts (Portaria n° 3 - DGO 22/02/1985) for the use of land located upstream and downstream of the dam. The purpose of the land concession agreement for agriculture and livestock was to settle farming families in the vicinity of the public dams. Confirming fossil data, the satellite image from 1985 clearly shows the impact of the law (Fig. 12, Table 1). Reforestation began in 1988, but the years 1990 to 1993 showed negative standard deviation of the annual mean precipitation, culminating in another severe drought in the year 1993. Here again, analyses of a satellite image acquired in 1991, which shows the return of a natural vegetation cover and a reduction in the extent of bare soil, support the significant

rise in tree pollen taxa (30–61%) mainly *M. caesalpinifolia* between 1990 and 1997 (Fig. 12, Table 1). In 1989, the return of vegetation cover was favored by the abandonment of cultivated land due to another law (National Institute for Colonization and Agrarian Reform INCRA Law 97.844 19/07/1989).

6. Conclusions

Our study demonstrates the possibility of reconstructing the disturbances caused by human activities and climatic changes in a hydrographic basin using sedimentary archives when historical data are inexistent, rare or damaged. Despite similar climate variability, major differences were observed between the two sites due to specific local human occupation and development policies. The ability to monitor these trends at a variety of scales provides crucial information for sustainable resource management decisions that are essential for the maintenance and improvement of human wellbeing in the BSA (Wu, 2013). Three levels of changes were observed depending on the duration of their impact on the landscape, annual, decadal or pluridecadal. In the Acaraú basin, the high climatic variability in recent decades did not seem to affect the composition of the Caatinga vegetation due to its extremely high resilience. As models have difficulty predicting the response of this natural rainfall regime to increasing land and sea temperatures (Marengo and Bernasconi, 2015), accurate monitoring is

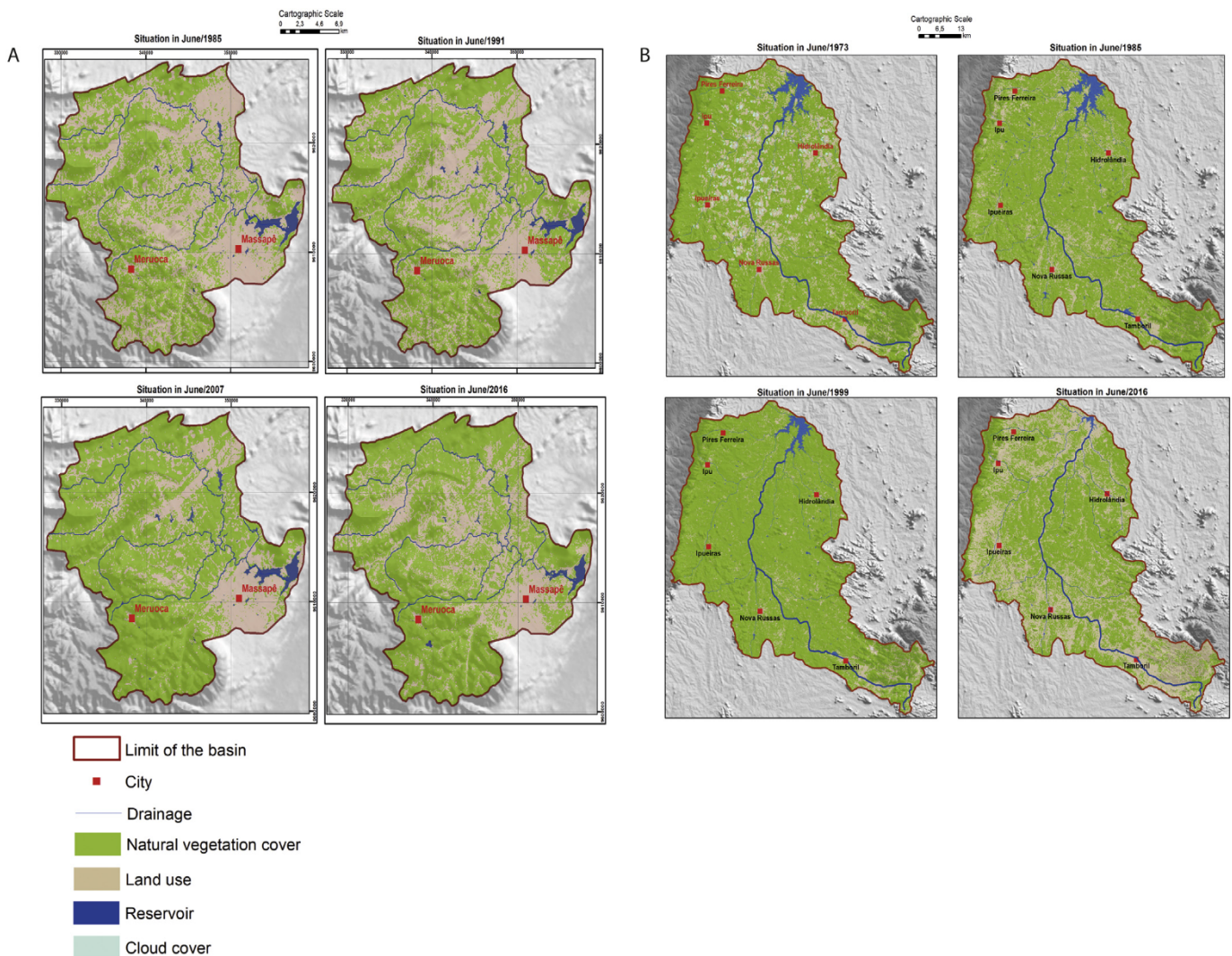


Fig. 12. Maps showing the vegetation cover. (A) In the Acaraú Mirim basin in 1985, 1991, 2007 and 2016, and (B) in the Araras basin in 1973, 1985, 1999 and 2016 extracted from Landsat imagery.

Table 1

Extent of natural vegetation, land use and reservoir from analysis of the satellite images acquired in the vicinity of ACA and ARA cores and presented in Fig. S11.

Year	Natural vegetation cover km ²	Land use km ²	Reservoir km ²
ACA			
1981	257.65	226.29	8.74
1985	290.81	193.6	8.29
2007	359.65	124.53	8.49
2016	343.44	144.09	5.13
ARA			
1973	2643.96	714.15	66.55
1985	2821.7	606.5	95.54
1999	3141.96	324	53.51
2016	2155.39	1353.39	11.81

needed before appropriate solutions for both people and the environment can be proposed. We emphasize that public policies play a significant role in changes in the landscape and in resources in the long term, whereas interannual climate variability and gradual climate change have not affected the vegetation cover of the Caatinga in the last 60 years. It is now crucial to define new forms of management that account for the physical, societal and sustainability specificities of the BSA and, to promote sustainable land use when scarce water resources and increasing temperatures threaten all the living organisms in these extreme conditions.

Data availability

The sequences reported in this paper will be deposited at the French national data repository Cyber carothèque <https://cybercarotheque.fr/> with a link to PANGAEA data base.

Fundings

This research was funded by a “sciences without boarder” (Portuguese acronym CSF) project “Evolution of biodiversity loss of areas in desertification processes” (CNPq 400890-2014-3), INCT IN-TREE: Interdisciplinary and transdisciplinary studies in ecology and evolution (CNPq CAPES FAPESBA) and covered a visiting foreign professor fellowship for MPL at the Federal University of Ceara (UFC) in the frame of the CSF project (2014–2018) and a postdoctoral grant (CNPq/FUNCAP) for VJP at the UFC (2015–2017) and for FRGB (PNPD/CAPES Program) at the PPGERN-UFC (2017–2019). This research is also part of the Labex-CEBA.

CRediT authorship contribution statement

Marie-Pierre Ledru: Conceptualization, Writing - original draft, Writing - review & editing. **Vivian Jeske-Pieruschka:** Formal analysis, Writing - original draft, Writing - review & editing. **Laurent Bremond:** Resources, Writing - original draft, Writing - review & editing. **Anne-Lise Develle:** Formal analysis, Writing - original draft, Writing - review & editing. **Pierre Sabatier:** Formal analysis, Writing - original draft, Writing - review & editing. **Eduardo Sávio Passos Rodrigues Martins:** Resources, Writing - original draft, Writing - review & editing. **Manuel Rodrigues de Freitas Filho:** Formal analysis, Writing - original draft, Writing - review & editing. **Diógenes Passos Fontenele:** Formal analysis, Writing - original draft, Writing - review & editing. **Fabien Arnaud:** Writing - original draft, Writing - review & editing. **Charly Favier:** Methodology, Writing - original draft, Writing - review & editing. **Francisco Rony Gomes Barroso:** Formal analysis, Writing - original draft, Writing - review & editing. **Francisca Soares Araújo:** Conceptualization, Writing - original draft, Writing - review & editing.

Declaration of competing interest

The authors declare that they have no known competing financial interests or personal relationships that could have appeared to influence the work reported in this paper.

Acknowledgements

We are grateful to COGERH at Massapê, DENOCS and the fishermen of Varjota for letting us use their boats, Maria Iracema Lioiela for information about plants of the Caatinga and for permission to collect flowers at the herbarium for our reference pollen collection, Ligia Queiroz Matias for information about plant species in the semi-arid wetlands, Vaneicia Gomes for preparing some pollen slides, Sandrine Canal for welcoming and supervising the students in the pollen laboratory at ISEM.

Appendix A. Supplementary data

Supplementary data to this article can be found online at <https://doi.org/10.1016/j.scitotenv.2020.137989>.

References

- Albuquerque, U.P., et al., 2009. How ethnobotany can aid biodiversity conservation: reflections on investigations in the semi-arid region of NE Brazil. *Biodivers. Conserv.* 18, 127–150.
- Alexander, M.A., et al., 2018. Projected sea surface temperatures over the 21st century: changes in the mean, variability and extremes for large marine ecosystem regions of Northern Oceans. *Elem Sci Anth* 6, 9.
- Alves, J.M.B., Servain, J., Campos, J.N.B., 2009. Relationship between ocean climatic variability and rain-fed agriculture in northeast Brazil. *Clim. Res.* 38, 225–236.
- Andrade-Lima, D., 1981. The Caatinga dominium. *Rev. Bras. Bot.* 4, 149–153.
- Araújo Filho, J.A., 1997. Desenvolvimento Sustentado da Caatinga. (Circular Técnica, 13. Sobral: Embrapa).
- Arnaud, F., et al., 2002. Flood and earthquake disturbance of 210Pb geochronology (Lake Anterne, NW Alps). *Terra Nova* 14, 225–232.
- Bajard, M., et al., 2016. Erosion record in Lake La Thuile sediments evidences montane landscape dynamics through the Holocene. *The Holocene* 26, 350–364.
- Barbosa, H.A., Kumar, T.V.L., 2016. Influence of rainfall variability on the vegetation dynamics over Northeastern Brazil. *J. Arid Environ.* 12, 377–387.
- Boyin, H., et al., 2015. Extended Reconstructed Sea Surface Temperature (ERSST), Version 4. NOAA National Centers for Environmental Information <https://doi.org/10.7289/V5KD1VVF> [11/07/2019].
- Bruel, R., Sabatier, P., 2020. serac: a R package for ShortlivEd RAdionuclide Chronology of recent sediment cores <https://doi.org/10.31223/osf.io/f4yma>.
- Cardoso-Silva, S., de Lima Ferreira, P.A., Moschini-Carlos, V., et al., 2016. Temporal and spatial accumulation of heavy metals in the sediments at Paiva Castro reservoir (São Paulo, Brazil). *Environ. Earth Sci.* 75, 9. <https://doi.org/10.1007/s12665-015-4828-2>.
- Centro de Gestão e Estudos Estratégicos (CGEE), 2016. Land degradation neutrality: implications for Brazil (Brasília, DF).
- Centro de Gestão e Estudos Estratégicos (CGEE), 2017. *Parcerias Estratégicas. vol 22* (Brasília, DF).
- Coradin, L., Camillo, J., Pareyn, F.G.C., 2018. Espécies nativas da flora brasileira de valor econômico atual ou potencial: plantas para o futuro: região Nordeste. MMA, Brasília, DF <http://www.mma.gov.br/publicacoes/biodiversidade/category/142-serie-biodiversidade.html>.
- Costa, R.C., Araújo, F.S., Lima-Verde, L.W., 2007. Flora and life-form spectrum in an area of deciduous thorn woodland (Caatinga) in northeastern Brazil. *J. Arid Environ.* 68, 237–247.
- Davison, W., 1993. Iron and manganese in lakes. *Earth Sci. Rev.* 34, 119–163. [https://doi.org/10.1016/0012-8252\(93\)90029-7](https://doi.org/10.1016/0012-8252(93)90029-7).
- Deflandre, B., Mucci, A., Gagné, J.P., Guignard, C., Sundby, B., 2002. Early diagenetic processes in coastal marine sediments disturbed by a catastrophic sedimentation event. *Geochim. Cosmochim. Acta* 66, 2547–2558. [https://doi.org/10.1016/S0016-7037\(02\)00861-X](https://doi.org/10.1016/S0016-7037(02)00861-X).
- Elbaz-Poulichet, F., Sabatier, P., Dezileau, L., Freydyer, R., 2014. Sedimentary record of V, U, Mo and Mn in the Pierre-Blanche lagoon (Southern France) – evidence for a major anoxia event during the Roman period. *The Holocene* 24, 1384–1392. <https://doi.org/10.1177/0959683614540957>.
- Faegri, K., Iversen, J., 1975. *Textbook of Pollen Analysis*. Munksgaard, Copenhagen.
- Ferrenberg, S., Reed, S.C., Benalp, J., 2015. Climate change and physical disturbance cause similar community shifts in biological soil crusts. *Proc. Natl. Acad. Sci.* 112, 12116–12121.
- Goldberg, E.D., 1963. Geochronology with 210Pb. *Radioact. Dating. Int. Atom. Energy Ag. Vienna*, pp. 121–131.
- Gurgel, J.J.S., Fernando, C.H., 1994. Fisheries in semi-arid Northeast Brazil with special reference to the role of tilapias. *Int. Rev. Hydrobiol.* 79, 77–94.

- Heiri, O., Lotter, A.F., Lemcke, G., 2001. Loss on ignition as a method for estimating organic and carbonate content in sediments: reproducibility and comparability of results. *J. Paleolimnol.* 25, 101–110.
- Holdridge, L.R., 1967. Life zone ecology. Tropical Science Center, San José Costa Rica.
- Hounsou-gbo, G.A., Araujo, M., Bourlès, B., Veleda, D., Servain, J., 2015. Tropical Atlantic contributions to strong rainfall variability along the Northeast Brazilian coast. *Adv. Meteorol.* 2015, 1–13. <https://doi.org/10.1155/2015/902084>.
- IBGE, 2010. Atlas nacional do Brasil. Milton Santos, Rio de Janeiro.
- IPCC Chapter 3, 2018. Impacts of 1.5°C global warming on natural and human systems. In: Masson-Delmotte V, V., et al. (Eds.), Global Warming of 1.5°C. an IPCC Special Report on the Impacts of Global Warming of 1.5°C above Pre-Industrial Levels and Related Global Greenhouse Gas Emission Pathways, in the Context of Strengthening the Global Response to the Threat of Climate Change, Sustainable Development, and Efforts to Eradicate Poverty. World Meteorological Organization, Geneva, Switzerland.
- IPCC Climate Change Synthesis Report, 2014. Topic 2 future climate changes risks and impacts. Contribution of Working Groups I, II and III to the Fifth Assessment Report of the Intergovernmental Panel on Climate Change eds. Pachauri RK, Meyer LA (Geneva, Switzerland).
- Jansen, J.H.F., Van der Gaast, S.J., Koster, B., Vaars, A.J., 1998. CORTEX, a shipboard XRF-scanner for element analyses in split sediment cores. *Mar. Geol.* 151, 143–153. [https://doi.org/10.1016/S0025-3227\(98\)00074-7](https://doi.org/10.1016/S0025-3227(98)00074-7).
- Joly, C., et al., 1999. Evolution of the Brazilian phytogeography classification systems: implications for biodiversity conservation. *Ciência e Cultura* 51, 331–348.
- Kümmel, B., Raup, D., 1965. Handbook of Paleontological Techniques. Freeman, San Francisco, USA.
- Lebel, T., Panthou, G., Vischel, T., 2018. Au Sahel pas de retour à la normale après la “grande sécheresse”. 12/11/2018. The Conversation <https://theconversation.com/au-sahel-pas-de-retour-a-la-normale-apres-la-grande-secheresse-106548>.
- Levine, S.N., Lini, A., Ostrofsky, M.L., et al., 2012. The eutrophication of Lake Champlain's northeastern arm: insights from paleolimnological analyses. *J. Great Lakes Res.* 38, 35–48. <https://doi.org/10.1016/j.jglr.2011.07.007>.
- Lima, T.R.A., et al., 2018. Lignin composition is related to xylem embolism resistance and leaf life span in trees in a tropical semiarid climate. *New Phytol.* 219, 1252–1262.
- Marengo, J.A., Bernasconi, M., 2015. Regional differences in aridity/drought conditions over Northeast Brazil: present state and future projections. *Climate Change* 129, 103–115.
- Milliken, W., et al., 2018. Impact of management regime and frequency on the survival and productivity of four native tree species used for fuelwood and charcoal in the caatinga of northeast Brazil. *Biomass Bioenergy* 116, 18–25.
- Ministerio do Meio Ambiente, 2007. Atlas das áreas susceptíveis a desertificação do Brasil. Secretaria dos recursos hídricos. Universidade Federal da Paraíba. Marcos Oliveira Santane organizador, Brasília DF Brazil <http://www.mma.gov.br/component/k2/itemlist/category/55-caatinga?start=15> (11/07/2019).
- Miranda, M.M.B., Andrade, T.A.P., 1990. Fundamentos de Palinologia: principais tipos de polen do litoral cearense. Editora da Universidade Federal do Ceará, Fortaleza, Brazil.
- Neto, C.R.J., 2012. Os primórdios da organização do espaço territorial e da vila cearense – algumas notas. *Anais do Museu Paulista* 20, 133–163.
- Oksanen, J., Blanchet, F.G., Friendly, M., Kin dt R., Legendre P., McGlinn D, Minchin R.S., O'Hara R.B., Simpson, G.L., Solymos, P., Stevens H.H., Szoecs, E., Wagner H, 2018. *Vegan: Community Ecology Package*. R Package Version 2.5-1.
- Oliveira, P.P., Santos, F.A.R., 2014. *Prospecção palinológica em méis da Bahia*. Print Mídia, Feira de Santana, Brazil, p. 2014.
- Radaeski, J.N., et al., 2013. Pólen nas angiospermas: diversidade e evolução. Editora da ULBRA, Canoá, Brazil.
- RCPol – The Online Pollen Catalogs Network. <https://biss.pensoft.net/article/25658/>. Available in: <<http://chave.rcpol.org.br/>>.
- Reyss, J.L., Schmidt, S., Legeleux, F., Bonté, P., 1995. Large, low background well-type detectors for measurements of environmental radioactivity. *Nuclear Instruments and Methods in Physics Research Section A: Accelerators, Spectrometers, Detectors and Associated Equipment* 357, 391–397.
- Sabatier, P., Poulenard, J., Fanget, B., Reyss, J.-L., Anne-Lise Develle, A.-L., et al., 2014. Long-term relationships among pesticide applications, mobility, and soil erosion in a vineyard watershed. *Proc. Natl. Acad. Sci. U. S. A.* 111, 15599–15600. <https://doi.org/10.1073/pnas.1214111111>.
- Salgado-Labouriau, M.L., 1973. Contribuição à palinologia dos Cerrados. *Academia Brasileira de Ciências*, Rio de Janeiro, Brazil.
- Silva, F.H.M., Santos, F.A.R., Lima, L.C.L., 2016. *Flora polínica das caatingas: Estação Biológica de Canudos [Canudos, Bahia, Brasil] (Micron Bahia, Feira de Santana, Brazil)*. Stockmarr, J., 1971. Tablets with spores used in absolute pollen analysis. *Pollen & Spores* 13, 615–621.
- Tabosa, A.B., Matias, L.Q., Martins, F.R., 2012. Live fast and die young: the aquatic macrophyte dynamics in a temporary pool in the Brazilian semiarid region. *Aquat. Bot.* 102, 71–78.
- Umbanhowar, C.E.J., Mcgrath, M.J., 1998. Experimental production and analysis of microscopic charcoal from wood, leaves and grasses. *The Holocene* 8, 341–346.
- Wilhelm, B., et al., 2012. 1.4 kyrs of flash flood events in the Southern European Alps: implications for extreme precipitation patterns and forcing over the north western Mediterranean area. *Quat. Res.* 78, 1–12.
- Wirth, S.B., et al., 2013. Combining sedimentological, trace metal (Mn, Mo) and molecular evidence for reconstructing past water-column redox conditions: the example of meromictic Lake Cadagno (Swiss Alps). *Geochimica Cosmochimica Acta* 120, 220–238. <https://doi.org/10.1016/j.gca.2013.06.017>.
- Wu, J., 2013. Landscape sustainability science: ecosystem services and human wellbeing in changing landscapes. *Landsc. Ecol.* 28, 999–1023.
- Ximenes, A.V.S.F.M., Furtado, J.L.S., 2018. O projeto Araras Norte em meio a seca no sertão revelando as fragilidades dos perímetros irrigados implantados no semiárido nordestino. *Revista da Casa da Geografia de Sobral* 20, 3–18.
- Zhang, H., Huo, S., Yeager, K.M., Li, C., Xi, B., Zhang, J., He, Z., Ma, C., 2019. Apparent relationships between anthropogenic factors and climate change indicators and POPs deposition in a lacustrine system. *J. Environ. Sci. (China)* 83, 174–182. <https://doi.org/10.1016/j.jes.2019.03.024> (Epub 2019 Apr 3).